IEEE Access
Multidisciplinary | Rapid Review | Open Access Journal

SPECIAL SECTION ON BIG DATA LEARNING AND DISCOVERY

Received May 19, 2018, accepted June 19, 2018, date of publication June 26, 2018, date of current version July 19, 2018.

Digital Object Identifier 10.1109/ACCESS.2018.2850782

Finite-Time Synchronization of Chaotic Memristive Multidirectional Associative Memory Neural Networks and Applications in Image Encryption

WEIPING WANG[1,2,3,4], XIN YU[1,2], XIONG LUO[1,2], (Member, IEEE), AND JÜRGEN KURTHS[3,4]

[1]School of Computer and Communication Engineering, University of Science and Technology Beijing, Beijing 100083, China
[2]Beijing Key Laboratory of Knowledge Engineering for Materials Science, Beijing 100083, China
[3]Institute of Physics, Humboldt-University, 10099 Berlin, Germany
[4]Potsdam Institute for Climate Impact Research, 14473 Potsdam, Germany

Corresponding authors: Weiping Wang (weipingwangjt@ustb.edu.cn) and Xiong Luo (xluo@ustb.edu.cn)

This work was supported in part by the National Key Research and Development Program of China under Grant 2017YFB0702300, in part by the State Scholarship Fund of China Scholarship Council (CSC), in part by the National Natural Science Foundation of China under Grant 61603032 and Grant 61174103, in part by the Fundamental Research Funds for the Central Universities under Grant 06500025, and in part by the University of Science and Technology Beijing-National Taipei University of Technology Joint Research Program under Grant TW201705.

ABSTRACT Traditional biological neural networks lack the capability of reflecting variable synaptic weights when simulating associative memory of human brains. In this paper, we propose a novel memristive multidirectional associative memory neural networks (MAMNNs) model with mixed time-varying delays. More precisely, the proposed model is investigated with time-varying delays and distributed delays. Then, we design two kinds of delay-independent and delay-dependent controllers to analyze the problem of finite-time synchronization. Based on the drive-response concept and Lyapunov function, some sufficient criteria guaranteeing the finite-time synchronization of the drive-response system are derived. With the removal of certain constraints on the weight parameters, the results we obtained for synchronization are less conservative. To illustrate the chaotic characteristics of the memristive MAMNNs, an image encryption scheme is designed. Meanwhile, the effectiveness of the proposed theories is validated with numerical experiments.

INDEX TERMS Finite-time synchronization, image encryption, memristor, multidirection associative memory neural networks.

I. INTRODUCTION

Images play an important role in human life. With the rapid development of network communication, secure transfers of large amounts of image data have become a challenging task. Therefore, encryption technologies have become highly important tools. Recently, image encryption methods based on chaotic mapping have attracted the attention of many researchers in [1]–[4]. In [1], an encryption algorithm that uses the chaos based S-BOX was developed for secure and speed image encryption. A visually meaningful image encryption scheme based on the lift wavelet transformation was proposed in [2]. In [3], a chaotic system based image encryption scheme with identical encryption and decryption algorithm was analyzed. Meanwhile, the authors in [4] proposed a chaotic system for color image encryption by combining Logistic, Sine and Tent systems. Although the image encryption methods based on chaotic mapping have been widely developed, there are few studies of biological neural networks [5]–[12], especially for memristive neural networks (MNNs) [11], [12]. The problem of image encryption based on chaotic neural networks was studied in [5]–[7] and the methods of image encryption based on the synchronization were showed in [8]–[10]. Meanwhile, the authors presented a novel image encryption scheme employing the memristive hyperchaotic system, cellular automata and DNA sequence operations in [11]. In [12], a new memristive chaotic system was presented, and its dynamical behaviors were analyzed. Therefore, an image encryption scheme based on memristive chaotic sequences is still a substantial topic.

Memristors have typical non-linear characteristics, and they are employed to replace the fixed-value resistors [13] in artificial neural networks to form MNNs [14]–[16]. In recent years, the dynamic behaviors of MNNs were analyzed in [17]–[19], where the dynamic behaviors have been widely applied to associative memory [20], medical image processing [21], [22], etc.. Meanwhile, memristive bidirectional associative memory neural networks (BAMNNs) have been extensively studied in [23]–[27]. In addition, as an extension of BAMNNs, MAMNNs are similar to BAMNNs in structure. MAMNNs were proposed by Hagiwara [28] and the dynamic behaviors of MAMNNs have attracted great attention of many researchers in [29]–[31]. The authors proposed a multi-valued exponential associative memory model in [29], and they analyzed the stability of this model. A discrete-time MAMNNs model with varying-time delays was formulated in [30], in which the global exponential stability of the system was analyzed. The authors devised a method in [31], which can accurately detect nodes able to exert strong influence over the multilayer networks. However, there exist few literatures about memristive MAMNNs. Thus, it is significant to study the dynamic behaviors of memristive MAMNNs.

It is generally known that time delays are inevitable in the hardware implementation of MNNs due to the switching of amplifiers. Various types of time delays, such as time-varying delays [32], distributed delays [33] and mixed delays [34] are often considered. Meanwhile, stability and synchronization of chaotic systems play an important role due to their potential applications to image encryption [5]–[12], secure communication [35], secure image transmission [36], intelligent data analysis [37], etc.. However, in practical applications, it is desirable that a synchronization objective is realized in finite-time. In recent years, some results on the synchronization of chaotic MNNs were obtained in [38]–[41], but there are few studies about the finite-time synchronization of memristive MAMNNs. Therefore, it is meaningful to analyze the finite-time synchronization of chaotic memristive MAMNNs.

Motivated by the above discussions, the main contributions of this paper can be summarized in the following:

- We propose a novel memristive MAMNNs model with mixed time-varying delays. More precisely the proposed model is investigated with time-varying delays and distributed delays.
- We design two kinds of delay-independent and delay-dependent controllers to analyze the synchronization of the drive-response system.
- Sufficient criteria guaranteeing the finite-time synchronization of the drive-response system are derived based on the drive-response concept and Lyapunov function.
- With the removal of certain constraints on the weight parameters and discuss the cases in detail, we obtain less conservative results for the synchronization of the drive-response system.
- To illustrate the performance of the proposed criteria, an image encryption scheme based on chaotic memristive MAMNNs sequences is designed.

The rest of this paper is organized as follows. The proposed memeristive MAMNNs model with mixed delays is introduced with some preliminaries in Section 2. Sufficient criteria for ensuring finite-time synchronization of the drive-response system are described in section 3. An image encryption method based on chaotic sequences of memristive MAMNNs is designed in Section 4. Numerical examples are discussed in Section 5, while Section 6 concludes this paper.

II. MODEL DESCRIPTION AND PRELIMINARIES

In this section, we introduce the following memristive MAMNNs with mixed delays :

$$\begin{aligned}\frac{dx_{ki}(t)}{dt} &= I_{ki} - d_{ki}(x_{ki}(t))x_{ki}(t) \\ &+ \sum_{\substack{p=1,\\ p\neq k}}^{m}\sum_{j=1}^{n_p} a_{pjki}(x_{ki}(t))f_{pj}(x_{pj}(t)) \\ &+ \sum_{\substack{p=1,\\ p\neq k}}^{m}\sum_{j=1}^{n_p} b_{pjki}(x_{ki}(t))f_{pj}(x_{pj}(t-\tau_{pjki}(t))) \\ &+ \sum_{\substack{p=1,\\ p\neq k}}^{m}\sum_{j=1}^{n_p} c_{pjki}(x_{ki}(t))\int_{t-\rho(t)}^{t} f_{pj}(x_{pj}(s))ds, \qquad (1)\end{aligned}$$

where $x_{ki}(t)$ denotes the voltage of the *ith* neuron in the field k, m is the total number of fields and n_p corresponds to the number of neurons in the field p. $d_{ki}(x_{ki}(t))$, $a_{pjki}(x_{ki}(t))$, $b_{pjki}(x_{ki}(t))$ and $c_{pjki}(x_{ki}(t))$ denote the synptic connection weights. The time delays $\tau_{pjki}(t)$ and $\rho(t)$ are time-varying delays and distributed delay, respectively. $f_{ki}(x)$ is activation function. I_{ki} represents the external input constants of the *ith* neuron in the field k.

Throughout this paper, a column vector is defined as $col(x_{ki}) = (x_{11}, x_{12}, \cdots, x_{mn_m})^T$. $co[\underline{\xi}, \overline{\xi}]$ denotes the convex closure on $[\underline{\xi}, \overline{\xi}]$. In the Banach space, all sets of continuous functions are expressed as $C([-\tau, 0], R^n)$. Besides, the initial values of system (1) are given as follows : $\phi(s) = (\phi_{11}(s), \phi_{12}(s), \cdots, \phi_{mn_m}(s))^T \in C([-\tau, 0], R^n)$, in which $\tau = \max\limits_{1\leq p\leq m, p\neq k} \max\limits_{1\leq j\leq n_p} \{\tau_{pjki}(t), \rho(t)\}$.

Some notations are defined as follows:

$\overline{d}_{ki} = \max\{\acute{d}_{ki}, \grave{d}_{ki}\}$, $\underline{d}_{ki} = \min\{\acute{d}_{ki}, \grave{d}_{ki}\}$, $\overline{a}_{pjki} = \max\{\acute{a}_{pjki}, \grave{a}_{pjki}\}$, $\underline{a}_{pjki} = \min\{\acute{a}_{pjki}, \grave{a}_{pjki}\}$, $\overline{b}_{pjki} = \max\{\acute{b}_{pjki}, \grave{b}_{pjki}\}$, $\underline{b}_{pjki} = \min\{\acute{b}_{pjki}, \grave{b}_{pjki}\}$, $\overline{c}_{pjki} = \max\{\acute{c}_{pjki}, \grave{c}_{pjki}\}$, $\underline{c}_{pjki} = \min\{\acute{c}_{pjki}, \grave{c}_{pjki}\}$, $0 \leq \tau_{pjki}(t) \leq \tau_1$, $0 \leq \rho(t) \leq \rho_1$, $\dot{\tau}_{pjki}(t) \leq \tau_2 < 1$.

According to the features of memristors and the current-voltage characteristics, as well as the applied set-valued mapping theorem and the stochastic differential inclusion theorem, for convenience, we define:

$$co(d_{ki}(x_{ki}(t))) = \begin{cases} \acute{d}_{ki}, & |x_{ki}(t)| < \Gamma_{ki}, \\ co\{\acute{d}_{ki}, \grave{d}_{ki}\}, & |x_{ki}(t)| = \Gamma_{ki}, \\ \grave{d}_{ki}, & |x_{ki}(t)| > \Gamma_{ki}, \end{cases}$$

$$co(a_{pjki}(x_{ki}(t))) = \begin{cases} \acute{a}_{pjki}, & |x_{ki}(t)| < \Gamma_{ki}, \\ co\{\acute{a}_{pjki}, \grave{a}_{pjki}\}, & |x_{ki}(t)| = \Gamma_{ki}, \\ \grave{a}_{pjki}, & |x_{ki}(t)| > \Gamma_{ki}, \end{cases}$$

$$co(b_{pjki}(x_{ki}(t))) = \begin{cases} \acute{b}_{pjki}, & |x_{ki}(t)| < \Gamma_{ki}, \\ co\{\acute{b}_{pjki}, \grave{b}_{pjki}\}, & |x_{ki}(t)| = \Gamma_{ki}, \\ \grave{b}_{pjki}, & |x_{ki}(t)| > \Gamma_{ki}, \end{cases}$$

$$co(c_{pjki}(x_{ki}(t))) = \begin{cases} \acute{c}_{pjki}, & |x_{ki}(t)| < \Gamma_{ki}, \\ co\{\acute{c}_{pjki}, \grave{c}_{pjki}\}, & |x_{ki}(t)| = \Gamma_{ki}, \\ \grave{c}_{pjki}, & |x_{ki}(t)| > \Gamma_{ki}. \end{cases}$$

Obviously, $co\{\acute{d}_{ki}, \grave{d}_{ki}\} = [\underline{d}_{ki}, \overline{d}_{ki}]$, $co\{\acute{a}_{pjki}, \grave{a}_{pjki}\} = [\underline{a}_{pjki}, \overline{a}_{pjki}]$, $co\{\acute{b}_{pjki}, \grave{b}_{pjki}\} = [\underline{b}_{pjki}, \overline{b}_{pjki}]$ and $co\{\acute{c}_{pjki}, \grave{c}_{pjki}\} = [\underline{c}_{pjki}, \overline{c}_{pjki}]$, for $k, p = 1, 2, \cdots, m, p \neq k, i = 1, 2, \cdots, n_k, j = 1, 2, \cdots, n_p$. According to the above definitions, system (1) can be written as follows

$$\begin{aligned} \frac{dx_{ki}(t)}{dt} \in\ & I_{ki} - co(d_{ki}(x_{ki}(t)))x_{ki}(t) \\ & + \sum_{\substack{p=1,\\ p\neq k}}^{m}\sum_{j=1}^{n_p} co(a_{pjki}(x_{ki}(t)))f_{pj}(x_{pj}(t)) \\ & + \sum_{\substack{p=1,\\ p\neq k}}^{m}\sum_{j=1}^{n_p} co(b_{pjki}(x_{ki}(t)))f_{pj}(x_{pj}(t-\tau_{pjki}(t))) \\ & + \sum_{\substack{p=1,\\ p\neq k}}^{m}\sum_{j=1}^{n_p} co(c_{pjki}(x_{ki}(t)))\int_{t-\rho(t)}^{t} f_{pj}(x_{pj}(s))ds, \end{aligned} \tag{2}$$

or equivalently, there exist $\hat{d}_{ki}(x_{ki}(t)) \in co(d_{ki}(x_{ki}(t)))$, $\hat{a}_{pjki}(x_{ki}(t)) \in co(a_{pjki}(x_{ki}(t)))$, $\hat{b}_{pjki}(x_{ki}(t)) \in co(b_{pjki}(x_{ki}(t)))$ and $\hat{c}_{pjki}(x_{ki}(t)) \in co(c_{pjki}(x_{ki}(t)))$, such that

$$\begin{aligned} \frac{dx_{ki}(t)}{dt} =\ & I_{ki} - \hat{d}_{ki}(x_{ki}(t))x_{ki}(t) \\ & + \sum_{\substack{p=1,\\ p\neq k}}^{m}\sum_{j=1}^{n_p} \hat{a}_{pjki}(x_{ki}(t))f_{pj}(x_{pj}(t)) \\ & + \sum_{\substack{p=1,\\ p\neq k}}^{m}\sum_{j=1}^{n_p} \hat{b}_{pjki}(x_{ki}(t))f_{pj}(x_{pj}(t-\tau_{pjki}(t))) \\ & + \sum_{\substack{p=1,\\ p\neq k}}^{m}\sum_{j=1}^{n_p} \hat{c}_{pjki}(x_{ki}(t))\int_{t-\rho(t)}^{t} f_{pj}(x_{pj}(s))ds. \end{aligned} \tag{3}$$

In this paper, we consider system (2) or (3) as the drive system. Then the corresponding response system is described as follows:

$$\begin{aligned} \frac{dy_{ki}(t)}{dt} \in\ & I_{ki} + \mu_{ki}(t) - co(d_{ki}(y_{ki}(t)))y_{ki}(t) \\ & + \sum_{\substack{p=1,\\ p\neq k}}^{m}\sum_{j=1}^{n_p} co(a_{pjki}(y_{ki}(t)))f_{pj}(y_{pj}(t)) \\ & + \sum_{\substack{p=1,\\ p\neq k}}^{m}\sum_{j=1}^{n_p} co(b_{pjki}(y_{ki}(t)))f_{pj}(y_{pj}(t-\tau_{pjki}(t))) \\ & + \sum_{\substack{p=1,\\ p\neq k}}^{m}\sum_{j=1}^{n_p} co(c_{pjki}(y_{ki}(t)))\int_{t-\rho(t)}^{t} f_{pj}(y_{pj}(s))ds, \end{aligned} \tag{4}$$

or equivalently, there exist $\hat{d}_{ki}(y_{ki}(t)) \in co(d_{ki}(y_{ki}(t)))$, $\hat{a}_{pjki}(y_{ki}(t)) \in co(a_{pjki}(y_{ki}(t)))$, $\hat{b}_{pjki}(y_{ki}(t)) \in co(b_{pjki}(y_{ki}(t)))$ and $\hat{c}_{pjki}(y_{ki}(t)) \in co(c_{pjki}(y_{ki}(t)))$, such that

$$\begin{aligned} \frac{dy_{ki}(t)}{dt} =\ & I_{ki} + \mu_{ki}(t) - \hat{d}_{ki}(y_{ki}(t))y_{ki}(t) \\ & + \sum_{\substack{p=1,\\ p\neq k}}^{m}\sum_{j=1}^{n_p} \hat{a}_{pjki}(y_{ki}(t))f_{pj}(y_{pj}(t)) \\ & + \sum_{\substack{p=1,\\ p\neq k}}^{m}\sum_{j=1}^{n_p} \hat{b}_{pjki}(y_{ki}(t))f_{pj}(y_{pj}(t-\tau_{pjki}(t))) \\ & + \sum_{\substack{p=1,\\ p\neq k}}^{m}\sum_{j=1}^{n_p} \hat{c}_{pjki}(y_{ki}(t))\int_{t-\rho(t)}^{t} f_{pj}(y_{pj}(s))ds, \end{aligned} \tag{5}$$

where $\mu_{ki}(t)$ represent the appropriate control inputs and

$$co(d_{ki}(y_{ki}(t))) = \begin{cases} \acute{d}_{ki}, & |y_{ki}(t)| < \Gamma_{ki}, \\ co\{\acute{d}_{ki}, \grave{d}_{ki}\}, & |y_{ki}(t)| = \Gamma_{ki}, \\ \grave{d}_{ki}, & |y_{ki}(t)| > \Gamma_{ki}, \end{cases}$$

$$co(a_{pjki}(y_{ki}(t))) = \begin{cases} \acute{a}_{pjki}, & |y_{ki}(t)| < \Gamma_{ki}, \\ co\{\acute{a}_{pjki}, \grave{a}_{pjki}\}, & |y_{ki}(t)| = \Gamma_{ki}, \\ \grave{a}_{pjki}, & |y_{ki}(t)| > \Gamma_{ki}, \end{cases}$$

$$co(b_{pjki}(y_{ki}(t))) = \begin{cases} \acute{b}_{pjki}, & |y_{ki}(t)| < \Gamma_{ki}, \\ co\{\acute{b}_{pjki}, \grave{b}_{pjki}\}, & |y_{ki}(t)| = \Gamma_{ki}, \\ \grave{b}_{pjki}, & |y_{ki}(t)| > \Gamma_{ki}, \end{cases}$$

$$co(c_{pjki}(y_{ki}(t))) = \begin{cases} \acute{c}_{pjki}, & |y_{ki}(t)| < \Gamma_{ki}, \\ co\{\acute{c}_{pjki}, \grave{c}_{pjki}\}, & |y_{ki}(t)| = \Gamma_{ki}, \\ \grave{c}_{pjki}, & |y_{ki}(t)| > \Gamma_{ki}. \end{cases}$$

The initial values of system (4) are given as follows : $\Phi(s) = (\Phi_{11}(s), \Phi_{12}(s), \cdots, \Phi_{mn_m}(s))^T \in C([-\tau, 0], R^n)$, in which $\tau = \max\{\tau_1, \rho_1\}$.

We define the synchronization errors of the system as follows:

$$e_{ki}(t) = y_{ki}(t) - x_{ki}(t),$$

where the initial values are defined as follows: $\Psi(s) = \Phi(s) - \phi(s) = (\Psi_{11}(s), \Psi_{12}(s), \cdots, \Psi_{21}(s), \cdots, \Psi_{mn_m}(s))^T \in C([-\tau, 0], R^n)$, in which $\tau = \max\{\tau_1, \rho_1\}$.

Assumption 1: For $k = 1, 2, \cdots, m, i = 1, 2, \cdots, n_k$, $\forall s_1, s_2 \in R$ and $s_1 \neq s_2$, the activation function $f_{ki}(\cdot)$ is odd bounded and satisfies the Lipschitz condition

$$|f_{ki}(s_1) - f_{ki}(s_2)| \leq L_{ki}|s_1 - s_2|, \quad |f_{ki}(\cdot)| \leq F,$$

where L_{ki} and F are nonnegative constants.

Definition 1: The response system is said to be synchronized with drive system in finite-time, if under a suitable controller, there exists a constant $T > 0$ such that $\lim_{t\to T} e_{ki}(t) = 0$ and $e_{ki}(t) \equiv 0$, for $t \geq T$, where T is called the setting time.

Lemma 1: (Chain Rule). Suppose that $V(x) : R^n \to R$ is C-regular and $x(t) : [0, +\infty) \to R$ is absolutely continuous on any compact subinterval of $[0, +\infty)$. Then $V(x(t)) : [0, +\infty) \to R$ is differentiable for a.a.t$\in [0, +\infty)$, and we have

$$\frac{dV(x(t))}{dt} = \varpi(t)\dot{x}(t), \quad \forall \varpi(t) \in \partial V(x(t)).$$

Lemma 2: Assume that a continuous, positive-definite function $V(t)$ and real numbers $h > 0$ and $0 < \eta < 1$, such that

$$\dot{V}(t) \leq -hV^{\eta}(t), \quad t \geq t_0,\ V(t) \geq 0.$$

Then the synchronization error system is finite-time stable, i.e., $V(t)$ satisfies

$$V^{1-\eta}(t) \leq V^{1-\eta}(t_0) - h(1-\eta)(t-t_0), \quad t_0 \leq t \leq T,$$

and $V(t) \equiv 0$ for $\forall t \geq T$, with the setting time T given by

$$T = t_0 + \frac{V^{1-\eta}(t_0)}{h(1-\eta)}.$$

III. MAIN RESULTS

In this section, some sufficient criteria guaranteeing the synchronization of the drive-response system are derived.

A. DELAY-INDEPENDENT CONTROLLER

In this subsection, we investigate the synchronization of the drive system (2) and the response system (4) with mixed delays. We design a delay-independent controller as follows:

$$\mu_{ki}(t) = -\delta_{ki}e_{ki}(t) - \theta_{ki}sign(e_{ki}(t)) - \frac{1}{2}sign(e_{ki}(t))h|e_{ki}(t)|^{\eta-1}, \quad (6)$$

where δ_{ki} and θ_{ki} are constants determined later, and the real numbers h and η satisfy $h > 0$ and $0 < \eta < 1$.

Theorem 1: Suppose that Assumption 1 holds. Then under the control law (6), the response system (4) can synchronize with the drive system (2) in finite-time

$$T = \frac{[V(0)]^{1-\eta}}{h(1-\eta)},$$

where $\delta_{ki} \geq \max\Big\{-\acute{d}_{ki} + \frac{1}{2}\sum_{\substack{p=1,\\ p\neq k}}^{m}\sum_{j=1}^{n_p}\Big[\acute{a}^2_{pjki}L^2_{pj} + 1 + \acute{b}^2_{pjki}L^2_{pj} + \rho_1\acute{c}^2_{pjki}L^2_{pj} + \frac{1}{1-\tau_2} + \rho_1\Big], -\grave{d}_{ki} + \frac{1}{2}\sum_{\substack{p=1,\\ p\neq k}}^{m}\sum_{j=1}^{n_p}\Big[\grave{a}^2_{pjki}L^2_{pj} + 1 + \grave{b}^2_{pjki}L^2_{pj} + \rho_1\grave{c}^2_{pjki}L^2_{pj} + \frac{1}{1-\tau_2} + \rho_1\Big]\Big\}$, $\theta_{ki} \geq |\acute{d}_{ki} - \grave{d}_{ki}|\Gamma_{ki} + \sum_{\substack{p=1,\\ p\neq k}}^{m}\sum_{j=1}^{n_p}\Big[|\acute{a}_{pjki} - \grave{a}_{pjki}|L_{pj}\Gamma_{pj} + |\acute{b}_{pjki} - \grave{b}_{pjki}|F + |\acute{c}_{pjki} - \grave{c}_{pjki}|\rho_1 F\Big]$, $V(0) = e^2_{ki}(0) + \frac{1}{1-\tau_2}\sum_{\substack{p=1,\\ p\neq k}}^{m}\sum_{j=1}^{n_p}\int_{-\tau_{pjki}(0)}^{0} e^2_{pj}(s)ds + \sum_{\substack{p=1,\\ p\neq k}}^{m}\sum_{j=1}^{n_p}\int_{-\rho_1}^{0}\int_{s}^{0} e^2_{pj}(z)dzds$, $h > 0$ and $0 < \eta < 1$.

Proof: Please see Appendix A.

Corollary 1: Suppose that Assumption 1 holds. Then under the control law (6), the response system (4) can synchronize with the drive system (2) in finite-time

$$T = \frac{[V(0)]^{1-\eta}}{h(1-\eta)},$$

where $\delta_{ki} \geq \max\Big\{-\acute{d}_{ki} + \frac{1}{2}\sum_{\substack{p=1,\\ p\neq k}}^{m}\sum_{j=1}^{n_p}\Big[\acute{a}^2_{pjki}L^2_{pj} + 1 + \acute{b}^2_{pjki}L^2_{pj} + \frac{1}{1-\tau_2}\Big], -\grave{d}_{ki} + \frac{1}{2}\sum_{\substack{p=1,\\ p\neq k}}^{m}\sum_{j=1}^{n_p}\Big[\grave{a}^2_{pjki}L^2_{pj} + 1 + \grave{b}^2_{pjki}L^2_{pj} + \frac{1}{1-\tau_2}\Big]\Big\}$, $\theta_{ki} \geq |\acute{d}_{ki} - \grave{d}_{ki}|\Gamma_{ki} + \sum_{\substack{p=1,\\ p\neq k}}^{m}\sum_{j=1}^{n_p}\Big[|\acute{a}_{pjki} - \grave{a}_{pjki}|L_{pj}\Gamma_{pj} + |\acute{b}_{pjki} - \grave{b}_{pjki}|F\Big]$, $h > 0$, $0 < \eta < 1$ and $V(0) = e^2_{ki}(0) + \frac{1}{1-\tau_2}\sum_{\substack{p=1,\\ p\neq k}}^{m}\sum_{j=1}^{n_p}\int_{-\tau_{pjki}(0)}^{0} e^2_{pj}(s)ds$.

Proof: Let the distributed delay $\rho(t) = 0$. The process of the proof is similar to Theorem 1, so it is omitted here.

Remark 1: There are some previous related works about synchronization of MNNs under the following conditions [42], [43]:

$$\begin{aligned}
&co[\underline{d}_{ki}, \overline{d}_{ki}]y_{pj}(t) - co[\underline{d}_{ki}, \overline{d}_{ki}]x_{pj}(t)\\
&\subseteq co[\underline{d}_{ki}, \overline{d}_{ki}](y_{pj}(t) - x_{pj}(t)), co[\underline{a}_{pjki}, \overline{a}_{pjki}]f_{pj}(y_{pj}(t))\\
&\quad - co[\underline{a}_{pjki}, \overline{a}_{pjki}]f_{pj}(x_{pj}(t))\\
&\subseteq co[\underline{a}_{pjki}, \overline{a}_{pjki}](f_{pj}(y_{pj}(t)) - f_{pj}(x_{pj}(t))),\\
&\quad co[\underline{b}_{pjki}, \overline{b}_{pjki}]f_{pj}(y_{pj}(t - \tau_{pjki}(t)))\\
&\quad - co[\underline{b}_{pjki}, \overline{b}_{pjki}]f_{pj}(x_{pj}(t - \tau_{pjki}(t)))\\
&\subseteq co[\underline{b}_{pjki}, \overline{b}_{pjki}](f_{pj}(y_{pj}(t - \tau_{pjki}(t)))\\
&\quad - f_{pj}(x_{pj}(t - \tau_{pjki}(t)))), co[\underline{c}_{pjki}, \overline{c}_{pjki}]\int_{t-\rho(t)}^{t} f_{pj}(y_{pj}(s))ds\\
&\quad - co[\underline{c}_{pjki}, \overline{c}_{pjki}]\int_{t-\rho(t)}^{t} f_{pj}(x_{pj}(s))ds\\
&\subseteq co[\underline{c}_{pjki}, \overline{c}_{pjki}](\int_{t-\rho(t)}^{t} f_{pj}(y_{pj}(s))ds - \int_{t-\rho(t)}^{t} f_{pj}(x_{pj}(s))ds).
\end{aligned}$$

It is easily checked that when $x_{ki}(t)$ and $y_{ki}(t)$ have same signs, or $x_{ki}(t) = 0$ or $y_{ki}(t) = 0$, the above conditions hold. Moreover, the results obtained in [42] and [43] are independent on the switching jumps Γ_{ki}. Hence, in this paper, with the removal of these strict conditions, the results we obtained are less conservative.

Remark 2: In the controllers 6, the discontinuous terms $sign(e_{ki}(t))$ may be undesirable in some practical applications. In this case, the continuous terms $\frac{e_{ki}(t)}{|e_{ki}(t)|+a}$ can be

chosen as approximations of $sign(e_{ki}(t))$, in which $a > 0$ is sufficiently small.

B. DELAY-DEPENDENT CONTROLLER

In this subsection, we investigate the synchronization of the drive system (2) and the response system (4) with mixed delays. We design a delay-dependent controller as follows:

$$\begin{aligned}\mu_{ki}(t) = &-\delta_{ki}e_{ki}(t) - \theta_{ki}sign(e_{ki}(t))|e_{pj}(t-\tau_{pjki}(t))| \\ &- \varepsilon_{ki}sign(e_{ki}(t))|\int_{t-\rho(t)}^{t} e_{pj}(s)ds| \\ &- sign(e_{ki}(t))(\gamma_{ki} + h|e_{ki}(t)|^{\eta}),\end{aligned} \tag{7}$$

where δ_{ki}, θ_{ki}, ε_{ki} and γ_{ki} are constants determined later, real numbers h and η satisfy $h > 0$ and $0 < \eta < 1$.

Theorem 2: Suppose that Assumption 1 holds. Then under the control law (7), the response system (4) can synchronize with the drive system (2) in finite-time

$$T = \frac{[V(0)]^{1-\eta}}{h(1-\eta)},$$

where $\delta_{ki} \geq \max\sum_{\substack{p=1,\\ p\neq k}}^{m}\sum_{j=1}^{n_p}\Big\{ -\acute{d}_{ki} + \acute{a}_{pjki}L_{pj}, -\grave{d}_{ki} + \grave{a}_{pjki}L_{pj}\Big\}$, $\theta_{ki} \geq \max\sum_{\substack{p=1,\\ p\neq k}}^{m}\sum_{j=1}^{n_p}\Big\{\acute{b}_{pjki}L_{pj}, \grave{b}_{pjki}L_{pj}\Big\}$, $\varepsilon_{ki} \geq \max\sum_{\substack{p=1,\\ p\neq k}}^{m}\sum_{j=1}^{n_p}\Big\{\acute{c}_{pjki}L_{pj}, \grave{c}_{pjki}L_{pj}\Big\}$, $\gamma_{ki} > |\acute{d}_{ki} - \grave{d}_{ki}|\Gamma_{ki} + \sum_{\substack{p=1,\\ p\neq k}}^{m}\sum_{j=1}^{n_p}\Big[|\acute{a}_{pjki} - \grave{a}_{pjki}|L_{pj}\Gamma_{pj} + |\acute{b}_{pjki} - \grave{b}_{pjki}|F + |\acute{c}_{pjki} - \grave{c}_{pjki}|\rho_1 F\Big]$, $h > 0$, $0 < \eta < 1$ and $V(0) = sign(e_{ki}(0))e_{ki}(0)$.

Proof: Please see Appendix B.

Corollary 2: Suppose that Assumption 1 holds. Then under the control law $\mu_{ki}(t) = -\delta_{ki}e_{ki}(t) - \theta_{ki}sign(e_{ki}(t))|e_{pj}(t-\tau_{pjki}(t))| - sign(e_{ki}(t))(\gamma_{ki}+h|e_{ki}(t)|^{\eta})$, the response system (4) can synchronize with the drive system (2) in finite-time

$$T = \frac{[V(0)]^{1-\eta}}{h(1-\eta)},$$

where $\delta_{ki} \geq \max\sum_{\substack{p=1,\\ p\neq k}}^{m}\sum_{j=1}^{n_p}\Big\{-\acute{d}_{ki} + \acute{a}_{pjki}L_{pj}, -\grave{d}_{ki} + \grave{a}_{pjki}L_{pj}\Big\}$, $\theta_{ki} \geq \max\sum_{\substack{p=1,\\ p\neq k}}^{m}\sum_{j=1}^{n_p}\Big\{\acute{b}_{pjki}L_{pj}, \grave{b}_{pjki}L_{pj}\Big\}$, $\gamma_{ki} > |\acute{d}_{ki} - \grave{d}_{ki}|\Gamma_{ki} + \sum_{\substack{p=1,\\ p\neq k}}^{m}\sum_{j=1}^{n_p}\Big[|\acute{a}_{pjki} - \grave{a}_{pjki}|L_{pj}\Gamma_{pj} + |\acute{b}_{pjki} - \grave{b}_{pjki}|F\Big]$, $h > 0$, $0 < \eta < 1$ and $V(0) = sign(e_{ki}(0))e_{ki}(0)$.

Proof: Let the distributed delay $\rho(t) = 0$. The process of the proof is similar to Theorem 2, so it is omitted here.

Remark 3: Theorem 1 takes into account the influence of delay-independent controllers on system synchronization, while Theorem 2 considers the influence of delay-dependent controllers on system stability. The two theorems show the importance of controllers for the system synchronization.

Remark 4: Due to the state of the neuron is not only related to itself, but also the changes in the neuron associated with it will have an impact on it. Therefore, in Theorem 2, we consider the delay-dependent control strategy.

IV. IMAGE ENCRYPTION

Image encryption technologies play an important role in transmitting large amounts of image data. In this section, we propose an image encryption algorithm based on the chaotic memristive MAMNNs obtained in Main Results. The specific steps of the algorithm are as follows:

1) Read the original color image, its size is $m * n * 3$.
2) Use the Mchange and Nchange functions to perform row permutation and column permutation for the image, respectively.
3) Trichromatic separation.
   - The R, G and B components of the image are separated, and their respective matrices are $I_R = image(:, :, 1)$, $I_G = image(:, :, 2)$ and $I_B = image(:, :, 3)$ respectively.
4) Generate three chaotic sequences.
   - According to the Corollary 1, we choose appropriate parameters and layers of the drive system, then we obtain three chaotic sequences $yint(1, m * n)$, $yint(2, m*n)$ and $yint(3, m*n)$ from different fields of memristive MAMNNs, respectively.
   - In order to make the numerical values of chaotic sequences between 0 and 255, the following operations are performed to the chaotic sequences $yint(j, m * n)$, where $j = 1, 2, 3$. (See Table 1.)

TABLE 1. Chaotic sequence $yint(j, m * n)$.

chaotic sequence $yint(j, m * n)$.

```
x=zeros(3,m*n);
for j=1:3
   for i=1:m*n
      if round(10*yint(j,i))<10*yint(j,i)
         x(j,i)=mod(round(10^8*(10*yint(j,i)-round(10*yint(j,i)))),256);
      else
         x(j,i)=mod(round(10^8*(1-(10*yint(j,i)-round(10*yint(j,i))))),256);
      end
   end
end
```

   - The three primary color matrices obtained in step 2 are converted into a one-dimensional matrix, respectively. Then we obtain three one-dimensional matrices $image_R = I_R(:)'$, $image_G = I_G(:)'$ and $iamge_B = I_B(:)'$.
5) Image encryption.
   - Perform the XOR operations on the three chaotic sequences $yint(j, m * n)(j = 1, 2, 3)$ and image sequences. The encrypted image is found in Table 2.
6) Trichromatic combination.

TABLE 2. XOR operation.

XOR operation.
for i=1:m*n
$a(i) = bitxor(x(1,i), image_R(i));$
$b(i) = bitxor(x(2,i), image_G(i));$
$c(i) = bitxor(x(3,i), image_B(i));$
end

- The three components R, G, B are combined and normalized by $image(:,:,1) = reshape(a, m, n)$, $image(:,:,2) = reshape(b, m, n)$, $image(:,:,3) = reshape(c, m, n)$ and $image = mat2gray(image)$.

V. NUMERICAL SIMULATION

In this section, several numerical examples are given to illustrate the effectiveness of our proposed synchronization criteria.

Example 1: We consider the following memristive MAMNNs with mixed delays. There are three fields and one neuron in each field.

$$\begin{aligned}\frac{dx_{k1}(t)}{dt} &= I_{k1} - d_{k1}(x_{k1}(t))x_{k1}(t) \\ &+ \sum_{\substack{p=1,\\ p\neq k}}^{3} a_{p1k1}(x_{k1}(t))f_{p1}(x_{p1}(t)) \\ &+ \sum_{\substack{p=1,\\ p\neq k}}^{3} b_{p1k1}(x_{k1}(t))f_{p1}(x_{p1}(t-\tau_{p1k1}(t))) \\ &+ \sum_{\substack{p=1,\\ p\neq k}}^{3} c_{p1k1}(x_{k1}(t))\int_{t-\rho(t)}^{t} f_{p1}(x_{p1}(s))ds,\end{aligned}$$

where

$$d_{11}(x_{11}(t)) = \begin{cases}1.3, & |x_{11}| \le \Gamma_{11},\\ 1.4, & |x_{11}| > \Gamma_{11},\end{cases}$$

$$d_{21}(x_{21}(t)) = \begin{cases}0.1, & |x_{11}| \le \Gamma_{21},\\ 0.2, & |x_{11}| > \Gamma_{21},\end{cases}$$

$$d_{31}(x_{31}(t)) = \begin{cases}0.3, & |x_{31}| \le \Gamma_{31},\\ 0.4, & |x_{31}| > \Gamma_{31},\end{cases}$$

$$a_{1121}(x_{21}(t)) = \begin{cases}-0.45, & |x_{21}(t)| \le \Gamma_{21},\\ 0.32, & |x_{21}(t)| > \Gamma_{21},\end{cases}$$

$$a_{1131}(x_{31}(t)) = \begin{cases}0.36, & |x_{31}(t)| \le \Gamma_{31},\\ 0.38, & |x_{31}(t)| > \Gamma_{31},\end{cases}$$

$$a_{2111}(x_{11}(t)) = \begin{cases}-1.1, & |x_{11}(t)| \le \Gamma_{11},\\ 1.24, & |x_{11}(t)| > \Gamma_{11},\end{cases}$$

$$a_{2131}(x_{31}(t)) = \begin{cases}1.14, & |x_{31}(t)| \le \Gamma_{31},\\ 0.32, & |x_{31}(t)| > \Gamma_{31},\end{cases}$$

$$a_{3111}(x_{11}(t)) = \begin{cases}1.2, & |x_{11}(t)| \le \Gamma_{11},\\ 1.18, & |x_{11}(t)| > \Gamma_{11},\end{cases}$$

$$a_{3121}(x_{21}(t)) = \begin{cases}-0.28, & |x_{21}(t)| \le \Gamma_{21},\\ 0.12, & |x_{21}(t)| > \Gamma_{21},\end{cases}$$

$$b_{1121}(x_{21}(t)) = \begin{cases}0.32, & |x_{21}(t)| \le \Gamma_{21},\\ 0.24, & |x_{21}(t)| > \Gamma_{21},\end{cases}$$

$$b_{1131}(x_{31}(t)) = \begin{cases}-0.34, & |x_{31}(t)| \le \Gamma_{31},\\ 0.42, & |x_{31}(t)| > \Gamma_{31},\end{cases}$$

$$b_{2111}(x_{11}(t)) = \begin{cases}1.38, & |x_{11}(t)| \le \Gamma_{11},\\ 1.1, & |x_{11}(t)| > \Gamma_{11},\end{cases}$$

$$b_{2131}(x_{31}(t)) = \begin{cases}0.15, & |x_{31}(t)| \le \Gamma_{31},\\ -0.49, & |x_{31}(t)| > \Gamma_{31},\end{cases}$$

$$b_{3111}(x_{11}(t)) = \begin{cases}-0.38, & |x_{11}(t)| \le \Gamma_{11},\\ -0.95, & |x_{11}(t)| > \Gamma_{11},\end{cases}$$

$$b_{3121}(x_{21}(t)) = \begin{cases}-0.45, & |x_{21}(t)| \le \Gamma_{21},\\ -0.22, & |x_{21}(t)| > \Gamma_{21}.\end{cases}$$

$$c_{1121}(x_{21}(t)) = \begin{cases}-0.84, & |x_{21}(t)| \le \Gamma_{21},\\ 0.18, & |x_{21}(t)| > \Gamma_{21},\end{cases}$$

$$c_{1131}(x_{31}(t)) = \begin{cases}0.68, & |x_{31}(t)| \le \Gamma_{31},\\ 0.42, & |x_{31}(t)| > \Gamma_{31},\end{cases}$$

$$c_{2111}(x_{11}(t)) = \begin{cases}0.24, & |x_{11}(t)| \le \Gamma_{11},\\ -0.58, & |x_{11}(t)| > \Gamma_{11},\end{cases}$$

$$c_{2131}(x_{31}(t)) = \begin{cases}-0.62, & |x_{31}(t)| \le \Gamma_{31},\\ -0.44, & |x_{31}(t)| > \Gamma_{31},\end{cases}$$

$$c_{3111}(x_{11}(t)) = \begin{cases}-0.82, & |x_{11}(t)| \le \Gamma_{11},\\ -0.84, & |x_{11}(t)| > \Gamma_{11},\end{cases}$$

$$c_{3121}(x_{21}(t)) = \begin{cases}0.78, & |x_{21}(t)| \le \Gamma_{21},\\ 0.19, & |x_{21}(t)| > \Gamma_{21}.\end{cases}$$

Let $\Gamma_{11} = \Gamma_{21} = \Gamma_{31} = 1$. We set the action functions as $f_{ki}(x) = \tanh(x)$. The time-varying delays and distributed delays are $\tau_{pjki}(t) = 0.5\cos(t) + 0.5$ and $\rho(t) = 0.5\sin(t) + 0.5$, respectively. According to Assumption 1, we have $L_{ki} = L_{pj} = 1$, $F = 1$. By calculating, we get $\tau_1 = 1$, $\tau_2 = 0.5$ and $\rho_1 = 1$. The initial values are set as $[x_{11}(t), x_{21}(t), x_{31}(t)] = [1.05, 0.25, -0.75]$, $[y_{11}(t), y_{21}(t), y_{31}(t)] = [-0.3, 0.45, 0.2]$.

Fig.1 represents the drive system (2) and the response system (4). They have chaotic attractors with the initial values given above. Fig.2 depicts the state trajectories of the drive system (2) and the response system (4). According to the conditions of Theorem 1, the delay-independent controllers are set as $\mu_{11}(t) = -4e_{11}(t) - 5sign(e_{11}(t)) - \frac{1}{2}sign(e_{11}(t))|e_{11}(t)|^{-0.5}$, $\mu_{21}(t) = -3e_{21}(t) - 4sign(e_{21}(t)) - \frac{1}{2}sign(e_{21}(t))|e_{21}(t)|^{-0.5}$, $\mu_{31}(t) = -3e_{31}(t) - 3sign(e_{31}(t)) - \frac{1}{2}sign(e_{31}(t))|e_{31}(t)|^{-0.5}$. According to the conditions of Theorem 2, the delay-dependent controllers are set as $\mu_{11}(t) = -1.2e_{11}(t) - 1.2sign(e_{11}(t))|e_{pj}(t-\tau_{pj11}(t))| - 0.1sign(e_{11}(t))\,|\int_{t-\rho(t)}^{t} e_{pj}(s)ds| - sign(e_{11}(t))(5+|e_{11}(t)|^{0.5})$,

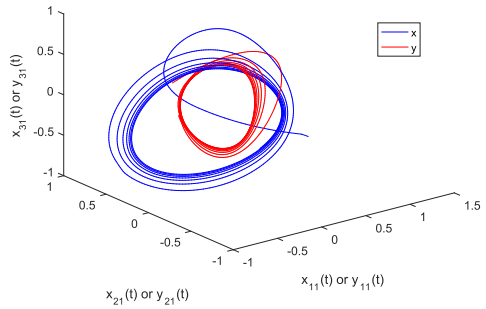

FIGURE 1. Phase trajectories of system (2)(corresponds to x) and system (4)(corresponds to y) with mixed delays.

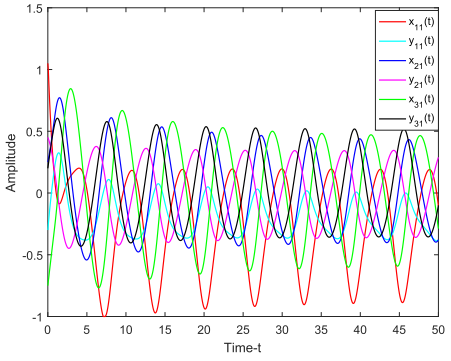

FIGURE 2. State trajectories of the drive system (2)(corresponds to x) and the response system (4)(corresponds to y).

$\mu_{21}(t) = -0.5e_{21}(t) - 0.1sign(e_{21}(t))|e_{pj}(t-\tau_{pj21}(t))| - 0.5sign(e_{21}(t))\,|\int_{t-\rho(t)}^{t} e_{pj}(s)ds| - sign(e_{21}(t))(4+|e_{21}(t)|^{0.5})$, $\mu_{31}(t) = -1.5e_{31}(t) - 0.1sign(e_{31}(t))|e_{pj}(t-\tau_{pj31}(t))| - 0.1sign(e_{31}(t))\,|\int_{t-\rho(t)}^{t} e_{pj}(s)ds| - sign(e_{31}(t))(3+|e_{31}(t)|^{0.5})$. Then (a-c) in Fig.3 describe the state trajectories of the errors system without controllers, with delay-independent and with delay-dependent controllers, respectively. It implies that the corresponding response system (4) can synchronize with the drive system (2) in finite-time, in which the setting time according to Theorem 1 is $T_{11} \approx 2.7$, $T_{21} \approx 0.4$ and $T_{31} =\approx 1.9$, the setting time according to Theorem 2 is $T_{21} \approx 2.3238$, $T22 \approx 0.8944$ and $T_{23} \approx 1.9494$.

Then we investigate system (2) and system (4) without distributed delays. Under the same parameters, Fig.4 represents the drive system (2) and the response system (4) without distributed delays. They have chaotic attractors with the initial values given above. Fig.5 depicts the state trajectories of system (2) and system (4). According to the conditions of Corollary 1, the delay-independent controllers are set as $\mu_{11}(t) = -3.5e_{11}(t) - 3.5sign(e_{11}(t)) - \frac{1}{2}sign(e_{11}(t))|e_{11}(t)|^{-0.5}$, $\mu_{21}(t) = -2.5e_{21}(t) - 2sign(e_{21}(t)) - \frac{1}{2}sign(e_{21}(t))|e_{21}(t)|^{-0.5}$, $\mu_{31}(t) = -2.5e_{31}(t) - 2.5sign(e_{31}(t)) - \frac{1}{2}sign(e_{31}(t))|e_{31}(t)|^{-0.5}$. According to the conditions of Corollary 2, the delay-dependent controllers are set as $\mu_{11}(t) = -1.2e_{11}(t) - 1.2sign(e_{11}(t))|e_{pj}(t-\tau_{pj11}(t))| - sign(e_{11}(t))(3.5 + |e_{11}(t)|^{0.5})$, $\mu_{21}(t) = -0.5e_{21}(t) - 0.1sign(e_{21}(t))|e_{pj}(t-\tau_{pj21}(t))| - sign(e_{21}(t))(2 + |e_{21}(t)|^{0.5})$, $\mu_{31}(t) = -1.5e_{31}(t) - 0.1sign(e_{31}(t))|e_{pj}(t-\tau_{pj31}(t))| - sign(e_{31}(t))(2.5 + |e_{31}(t)|^{0.5})$. Then (a-c) in Fig.6 describe the state trajectories of the errors system

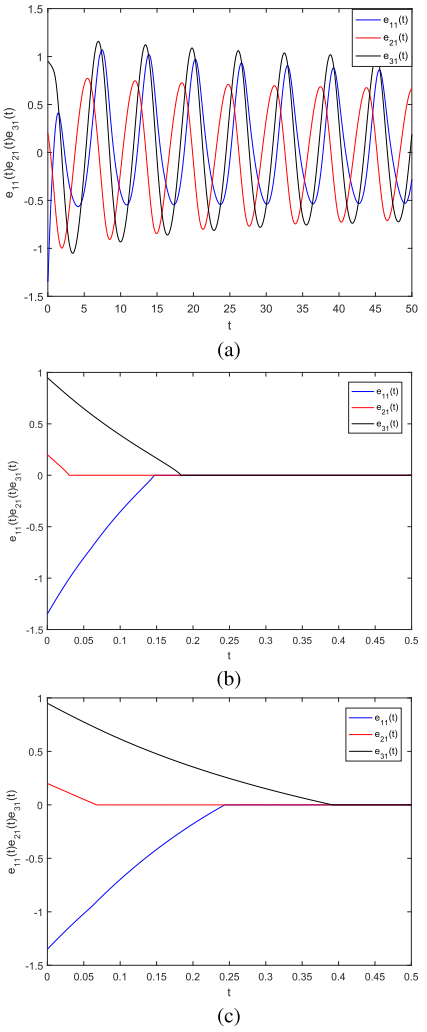

FIGURE 3. State trajectories of errors between the drive system (2) and the response system (4). (a) The errors without controllers. (b) The errors with delay-independent controllers. (c) The errors with delay-dependent controllers.

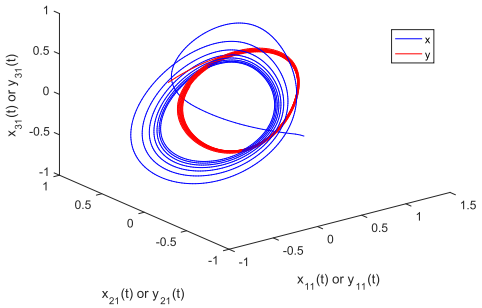

FIGURE 4. Phase trajectories of system (2)(corresponds to x) and system (4)(corresponds to y) without distributed delays.

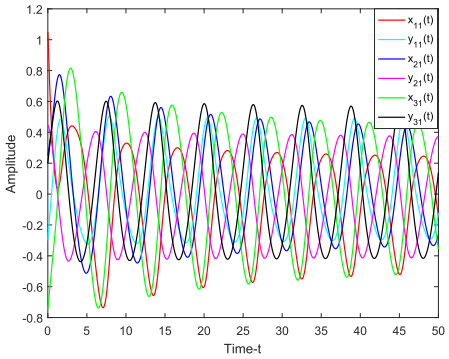

FIGURE 5. State trajectories of the drive system (2)(corresponds to x) and the response system (4)(corresponds to y) without distributed delays.

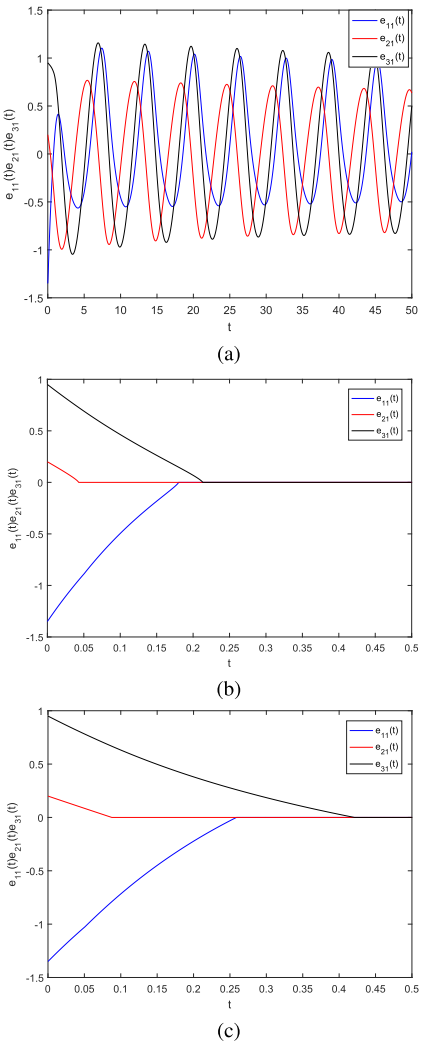

FIGURE 6. State trajectories of errors between system (2) and system (4) without distributed delays. (a) The errors without controllers. (b) The errors with delay-independent controllers. (c) The errors with delay-dependent controllers.

without controllers, with delay-independent and with delay-dependent controllers, respectively. It implies that the corresponding response system (4) can synchronize with the drive system (2) in finite-time.

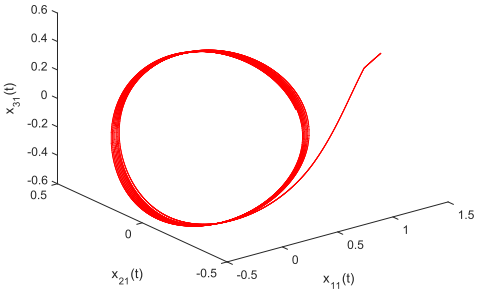

FIGURE 7. Phase trajectories of system (2) without distributed delays.

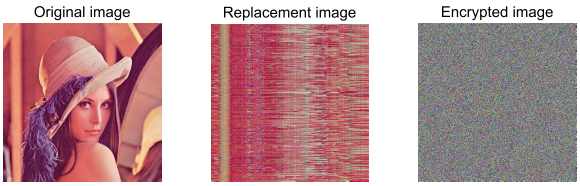

FIGURE 8. The process of encryption of an image.

Example 2: We consider the following memristive MAMNNs without distributed delays. There are three fields and one neuron in each field.

$$\begin{aligned}\frac{dx_{k1}(t)}{dt} &= I_{k1} - d_{k1}(x_{k1}(t))x_{k1}(t) \\ &\quad + \sum_{\substack{p=1,\\ p\neq k}}^{3} a_{p1k1}(x_{k1}(t))f_{p1}(x_{p1}(t)) \\ &\quad + \sum_{\substack{p=1,\\ p\neq k}}^{3} b_{p1k1}(x_{k1}(t))f_{p1}(x_{p1}(t-\tau_{p1k1}(t))),\end{aligned}$$

where the parameters are the same as in Example 1. The initial values are set as $[x_{11}(t), x_{21}(t), x_{31}(t)] = [1.2, -0.3, 0.4]$, and Fig.7 represents system (2) without distributed delays. It has chaotic attractor with the initial values.

Then we select a standard color image of the size of $512 * 512$ to encrypt the image (lena.tif) based on the memristive MAMNNs without distributed delays. Fig.8 describes the process of encryption of the original image. It can be seen that the encrypted image has lost the original image feature based on the given encryption method.

The gray histogram is a powerful attribute to describe the statistical characteristics of the image. Fig.9 displays the gray histogram of the original image, and it can be seen that there exist distribution characteristics in the gray histogram of the three components. Fig.10 describes the gray histogram of the encrypted image. It can be seen that the gray histogram of the three components is uniformly distributed. This implies that our encryption method can effectively encrypt the image.

Correlation analysis of adjacent pixels is an important indicator to evaluate the encryption effect of an image.

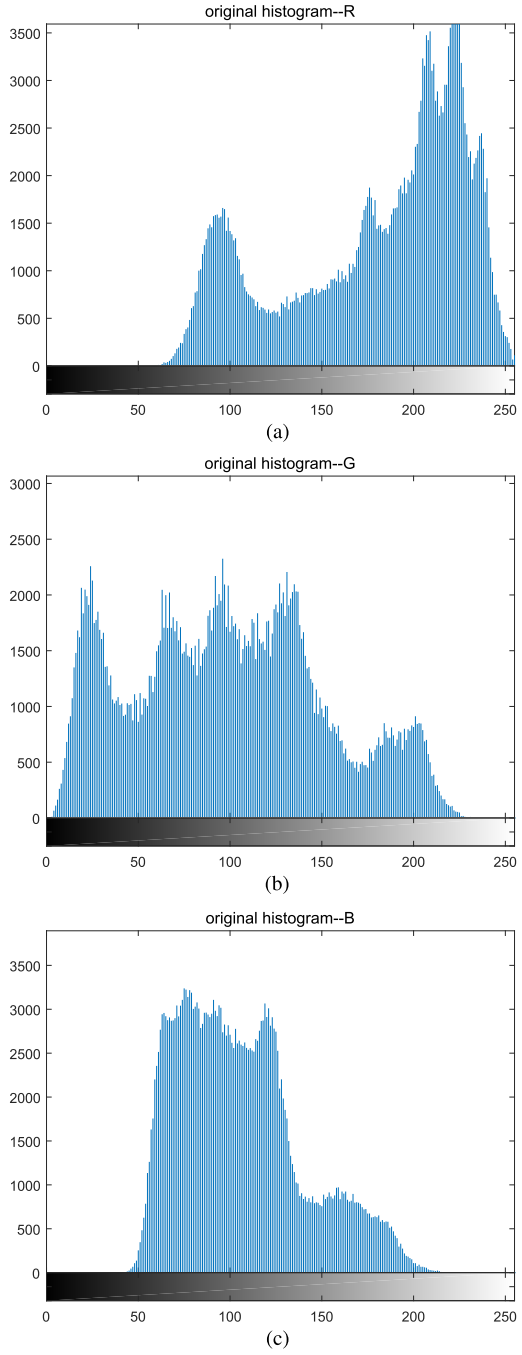

FIGURE 9. The histogram of the original image. (a) Original image—R component. (b) Original image—G component. (c) Original image—B component.

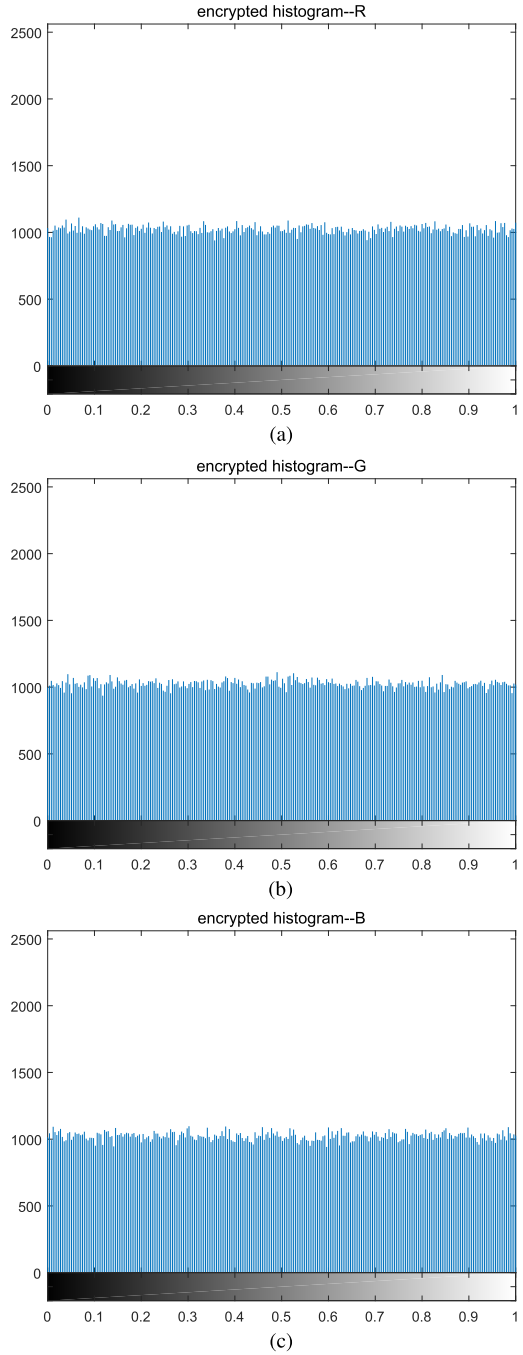

FIGURE 10. The histogram of the encrypted image. (a) Encrypted image—R component. (b) Encrypted image—G component. (c) Encrypted image—B component.

TABLE 3. Correlation analysis of adjacent pixel of the original image.

	The proposed.	Method in [44]	Replacement	Chaos
horizontal direction	0.9733	0.9663	0.9765	0.9717
vertical direction	0.9843	0.9780	0.9812	0.9821
diagonal direction	0.9623	0.9873	0.9644	0.9516

TABLE 4. Correlation analysis of adjacent pixel of the encrypted image.

	The proposed.	Method in [44]	Replacement	Chaos
horizontal direction	-0.0175	0.0234	0.0810	0.0151
vertical direction	0.0067	-0.0167	0.1816	-0.0155
diagonal direction	0.0052	-0.0172	-0.0231	-0.0139

We randomly select 1000 pairs of pixel values, in which Fig.11 shows the correlation analysis of adjacent pixels of the original image, Fig.12 describes the correlation analysis of adjacent pixels of the encrypted image. The specific correlation is shown in Table 3 and Table 4.

According to Table 3, we can see that the correlation coefficients of adjacent pixels of the original image are close to 1, i.e. it has a strong correlation. However, we can see that

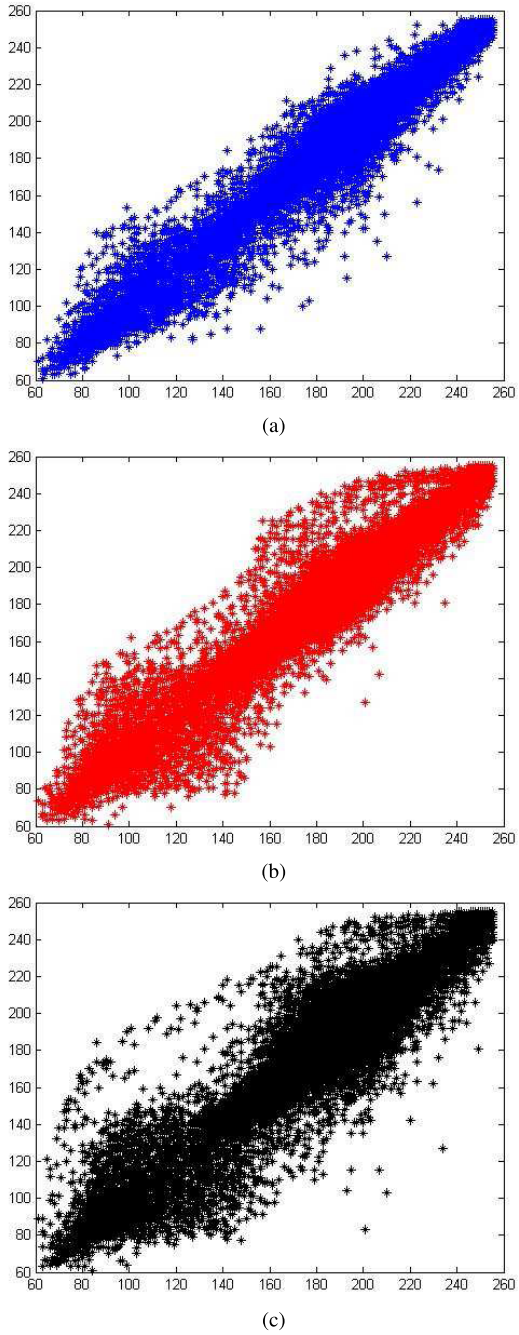

FIGURE 11. Correlation analysis of adjacent pixels of the original image. (a) Horizontal direction. (b) Vertical direction. (c) Diagonal direction.

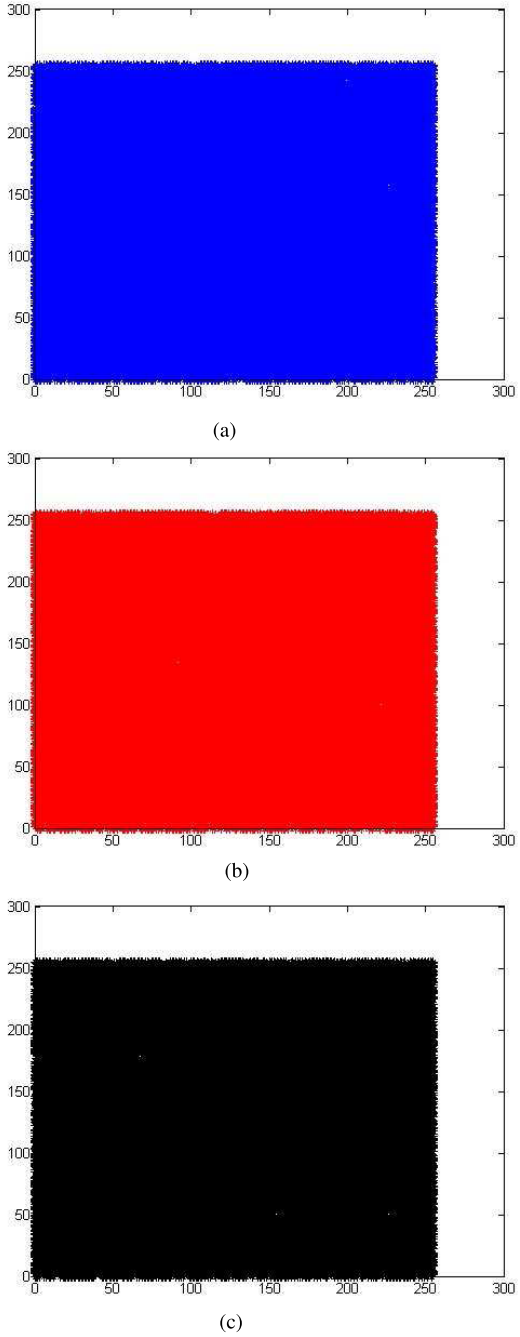

FIGURE 12. Correlation analysis of adjacent pixels of the encrypted image. (a) Horizontal direction. (b) Vertical direction. (c) Diagonal direction.

the correlation coefficients of adjacent pixels of the encrypted image are close to 0 in Table 4, i.e. they are almost irrelevant. This shows that our encryption method can effectively encrypt the image.

Compared with the results of literature [44], our proposed method has less correlation coefficients of adjacent pixels of the encrypted image, so it has better ability to encrypt images. At the same time, we combine the two encryption methods of replacement and chaos, which is more effective than using only one encryption method.

VI. CONCLUSION

In this paper, we propose a novel memristive MAMNNs model, which includes time-varying delays and distributed time delays. Then the finite-time synchronization of our proposed model is analyzed by creating appropriate controllers.

In the proposed approach, we obtain some less conservative results by removing certain strict conditions. By constructing a suitable Lyapunov function and using some inequality techniques, some sufficient criteria for guaranteeing the finite-time synchronization of the drive-response system are obtained. An image encryption scheme is designed based on the chaotic memristive MAMNNs. Furthermore, some numerical simulations are delivered to demonstrate the effectiveness of our proposed theories.

APPENDIX A
PROOF OF THEOREM 1

Construct the following Lyapunov function:

$$V(t) = e_{ki}^2(t) + \frac{1}{1-\tau_2}\sum_{\substack{p=1,\\ p\neq k}}^{m}\sum_{j=1}^{n_p}\int_{t-\tau_{pjki}(t)}^{t} e_{pj}^2(s)ds + \sum_{\substack{p=1,\\ p\neq k}}^{m}\sum_{j=1}^{n_p}\int_{-\rho_1}^{0}\int_{t+s}^{t} e_{pj}^2(z)dzds. \quad (8)$$

According to the differential inclusion theorem, Theorem 1 will be proved in nine cases.

① $|x_{ki}(t)| < \Gamma_{ki}$, $|y_{ki}(t)| < \Gamma_{ki}$.

The drive system (2) can be written as follows:

$$\frac{dx_{ki}(t)}{dt} = I_{ki} - \acute{d}_{ki}x_{ki}(t) + \sum_{\substack{p=1,\\ p\neq k}}^{m}\sum_{j=1}^{n_p}\acute{a}_{pjki}f_{pj}(x_{pj}(t)) + \sum_{\substack{p=1,\\ p\neq k}}^{m}\sum_{j=1}^{n_p}\acute{b}_{pjki}f_{pj}(x_{pj}(t-\tau_{pjki}(t))) + \sum_{\substack{p=1,\\ p\neq k}}^{m}\sum_{j=1}^{n_p}\acute{c}_{pjki}\int_{t-\rho(t)}^{t} f_{pj}(x_{pj}(s))ds. \quad (9)$$

The response system (4) can be written as follows:

$$\frac{dy_{ki}(t)}{dt} = I_{ki} - \acute{d}_{ki}y_{ki}(t) + \sum_{\substack{p=1,\\ p\neq k}}^{m}\sum_{j=1}^{n_p}\acute{a}_{pjki}f_{pj}(y_{pj}(t)) + \sum_{\substack{p=1,\\ p\neq k}}^{m}\sum_{j=1}^{n_p}\acute{b}_{pjki}f_{pj}(y_{pj}(t-\tau_{pjki}(t))) + \sum_{\substack{p=1,\\ p\neq k}}^{m}\sum_{j=1}^{n_p}\acute{c}_{pjki}\int_{t-\rho(t)}^{t} f_{pj}(y_{pj}(s))ds + \mu_{ki}(t). \quad (10)$$

Then the error system is obtained as follows:

$$\frac{de_{ki}(t)}{dt} = \mu_{ki}(t) - \acute{d}_{ki}e_{ki}(t) + \sum_{\substack{p=1,\\ p\neq k}}^{m}\sum_{j=1}^{n_p}\acute{a}_{pjki}\tilde{f}_{pj}(e_{pj}(t)) + \sum_{\substack{p=1,\\ p\neq k}}^{m}\sum_{j=1}^{n_p}\acute{b}_{pjki}\tilde{f}_{pj}(e_{pj}(t-\tau_{pjki}(t))) + \sum_{\substack{p=1,\\ p\neq k}}^{m}\sum_{j=1}^{n_p}\acute{c}_{pjki}\int_{t-\rho(t)}^{t}\tilde{f}_{pj}(e_{pj}(s))ds, \quad (11)$$

where $\tilde{f}_{pj}(e_{pj}(t)) = f_{pj}(y_{pj}(t)) - f_{pj}(x_{pj}(t))$, $\tilde{f}_{pj}(e_{pj}(t-\tau_{pjki}(t))) = f_{pj}(y_{pj}(t-\tau_{pjki}(t))) - f_{pj}(x_{pj}(t-\tau_{pjki}(t)))$, $\int_{t-\rho(t)}^{t}\tilde{f}_{pj}(e_{pj}(s))ds = \int_{t-\rho(t)}^{t}f_{pj}(y_{pj}(s))ds - \int_{t-\rho(t)}^{t}f_{pj}(x_{pj}(s))ds$.

Along the trajectory of system (11), we calculate the derivative as follows:

$$\begin{aligned}\dot{V}(t) = {} & 2e_{ki}(t)\Big[-\acute{d}_{ki}e_{ki}(t) + \sum_{\substack{p=1,\\ p\neq k}}^{m}\sum_{j=1}^{n_p}\acute{a}_{pjki}\tilde{f}_{pj}(e_{pj}(t)) + \mu_{ki}(t) + \sum_{\substack{p=1,\\ p\neq k}}^{m}\sum_{j=1}^{n_p}\acute{b}_{pjki}\tilde{f}_{pj}(e_{pj}(t-\tau_{pjki}(t))) \\ & + \sum_{\substack{p=1,\\ p\neq k}}^{m}\sum_{j=1}^{n_p}\acute{c}_{pjki}\int_{t-\rho(t)}^{t}\tilde{f}_{pj}(e_{pj}(s))ds\Big] + \frac{1}{1-\tau_2}\times\sum_{\substack{p=1,\\ p\neq k}}^{m}\sum_{j=1}^{n_p}e_{pj}^2(t) - \sum_{\substack{p=1,\\ p\neq k}}^{m}\sum_{j=1}^{n_p}e_{pj}^2(t-\tau_{pjki}(t)) \\ & + \sum_{\substack{p=1,\\ p\neq k}}^{m}\sum_{j=1}^{n_p}\rho_1 e_{pj}^2(t) - \sum_{\substack{p=1,\\ p\neq k}}^{m}\sum_{j=1}^{n_p}\int_{t-\rho(t)}^{t}e_{pj}^2(s)ds.\end{aligned} \quad (12)$$

According to Assumption 1, we obtain

$$\begin{aligned}\dot{V}(t) \le {} & -(2\acute{d}_{ki}+2\delta_{ki})e_{ki}^2(t) - 2\theta_{ki}|e_{ki}(t)| - h|e_{ki}(t)|^{\eta} + 2|e_{ki}(t)|\sum_{\substack{p=1,\\ p\neq k}}^{m}\sum_{j=1}^{n_p}\acute{a}_{pjki}L_{pj}|e_{pj}(t)| + 2|e_{ki}(t)| \\ & \times\sum_{\substack{p=1,\\ p\neq k}}^{m}\sum_{j=1}^{n_p}\acute{b}_{pjki}L_{pj}|e_{pj}(t-\tau_{pjki}(t))| + 2|e_{ki}(t)| \\ & \times\sum_{\substack{p=1,\\ p\neq k}}^{m}\sum_{j=1}^{n_p}\acute{c}_{pjki}L_{pj}\int_{t-\rho(t)}^{t}|e_{pj}(s)|ds + \frac{1}{1-\tau_2} \\ & \times\sum_{\substack{p=1,\\ p\neq k}}^{m}\sum_{j=1}^{n_p}e_{pj}^2(t) - \sum_{\substack{p=1,\\ p\neq k}}^{m}\sum_{j=1}^{n_p}e_{pj}^2(t-\tau_{pjki}(t)) \\ & + \sum_{\substack{p=1,\\ p\neq k}}^{m}\sum_{j=1}^{n_p}\rho_1 e_{pj}^2(t) - \sum_{\substack{p=1,\\ p\neq k}}^{m}\sum_{j=1}^{n_p}\int_{t-\rho(t)}^{t}e_{pj}^2(s)ds.\end{aligned} \quad (13)$$

By using the mean-value inequality, then we have

$$\begin{aligned}& 2|e_{ki}(t)|\acute{a}_{pjki}L_{pj}|e_{pj}(t)| \\ & \le \acute{a}_{pjki}^2L_{pj}^2e_{ki}^2(t) + e_{pj}^2(t),\ 2|e_{ki}(t)|\acute{b}_{pjki}L_{pj}|e_{pj}(t-\tau_{pjki}(t))| \\ & \le \acute{b}_{pjki}^2L_{pj}^2e_{ki}^2(t) + e_{pj}^2(t-\tau_{pjki}(t)),\ 2|e_{ki}(t)|\acute{c}_{pjki}L_{pj} \\ & \quad\times\int_{t-\rho(t)}^{t}|e_{pj}(s)|ds \\ & \le \rho_1\acute{c}_{pjki}^2L_{pj}^2e_{ki}^2(t) + \int_{t-\rho(t)}^{t}e_{pj}^2(s)ds.\end{aligned}$$

Then we get

$$\dot{V}(t) \le \Big[-2\acute{d}_{ki} - 2\delta_{ki} + \sum_{\substack{p=1,\\ p\neq k}}^{m}\sum_{j=1}^{n_p}(\acute{a}_{pjki}^2 L_{pj}^2 + \acute{b}_{pjki}^2 L_{pj}^2 + \rho_1 \acute{c}_{pjki}^2 L_{pj}^2 + 1 + \frac{1}{1-\tau_2} + \rho_1)\Big] e_{ki}^2(t) - 2\theta_{ki}|e_{ki}(t)| - h|e_{ki}(t)|^{\eta}. \quad (14)$$

Under the conditions of Theorem 1, we obtain

$$\dot{V}(t) \le -h|e_{ki}(t)|^{\eta}. \quad (15)$$

Then, according to Lemma 2, the drive system (2) and the response system (4) are synchronized in the finite-time $T = t_0 + \frac{V^{1-\eta}(t_0)}{h(1-\eta)}$. This implies the proof is completed.

② $|x_{ki}(t)| > \Gamma_{ki}$, $|y_{ki}(t)| > \Gamma_{ki}$.

The drive system (2) can be written as follows:

$$\frac{dx_{ki}(t)}{dt} = I_{ki} - \grave{d}_{ki}x_{ki}(t) + \sum_{\substack{p=1,\\ p\neq k}}^{m}\sum_{j=1}^{n_p}\grave{a}_{pjki}f_{pj}(x_{pj}(t)) + \sum_{\substack{p=1,\\ p\neq k}}^{m}\sum_{j=1}^{n_p}\grave{b}_{pjki}f_{pj}(x_{pj}(t-\tau_{pjki}(t))) + \sum_{\substack{p=1,\\ p\neq k}}^{m}\sum_{j=1}^{n_p}\grave{c}_{pjki}\int_{t-\rho(t)}^{t} f_{pj}(x_{pj}(s))ds. \quad (16)$$

The response system (4) can be written as follows:

$$\frac{dy_{ki}(t)}{dt} = I_{ki} - \grave{d}_{ki}y_{ki}(t) + \sum_{\substack{p=1,\\ p\neq k}}^{m}\sum_{j=1}^{n_p}\grave{a}_{pjki}f_{pj}(y_{pj}(t)) + \sum_{\substack{p=1,\\ p\neq k}}^{m}\sum_{j=1}^{n_p}\grave{b}_{pjki}f_{pj}(y_{pj}(t-\tau_{pjki}(t))) + \sum_{\substack{p=1,\\ p\neq k}}^{m}\sum_{j=1}^{n_p}\grave{c}_{pjki}\int_{t-\rho(t)}^{t} f_{pj}(y_{pj}(s))ds + \mu_{ki}(t). \quad (17)$$

Then the error system is obtained as follows:

$$\frac{de_{ki}(t)}{dt} = \mu_{ki}(t) - \grave{d}_{ki}e_{ki}(t) + \sum_{\substack{p=1,\\ p\neq k}}^{m}\sum_{j=1}^{n_p}\grave{a}_{pjki}\tilde{f}_{pj}(e_{pj}(t)) + \sum_{\substack{p=1,\\ p\neq k}}^{m}\sum_{j=1}^{n_p}\grave{b}_{pjki}\tilde{f}_{pj}(e_{pj}(t-\tau_{pjki}(t))) + \sum_{\substack{p=1,\\ p\neq k}}^{m}\sum_{j=1}^{n_p}\grave{c}_{pjki}\int_{t-\rho(t)}^{t}\tilde{f}_{pj}(e_{pj}(s))ds. \quad (18)$$

The proof of the rest is similar to ①, so it is omitted here.

③ $|x_{ki}(t)| < \Gamma_{ki}$, $|y_{ki}(t)| > \Gamma_{ki}$.

The drive system (2) can be written as system (9), the response system (4) can be written as system (17). Then the error system is obtained as follows:

$$\frac{de_{ki}(t)}{dt} = \mu_{ki}(t) - \grave{d}_{ki}e_{ki}(t) + \sum_{\substack{p=1,\\ p\neq k}}^{m}\sum_{j=1}^{n_p}\grave{a}_{pjki}\tilde{f}_{pj}(e_{pj}(t)) + \sum_{\substack{p=1,\\ p\neq k}}^{m}\sum_{j=1}^{n_p}\grave{b}_{pjki}\tilde{f}_{pj}(e_{pj}(t-\tau_{pjki}(t))) + \sum_{\substack{p=1,\\ p\neq k}}^{m}\sum_{j=1}^{n_p}\grave{c}_{pjki}\int_{t-\rho(t)}^{t}\tilde{f}_{pj}(e_{pj}(s))ds + (\acute{d}_{ki} - \grave{d}_{ki})x_{ki}(t) + \sum_{\substack{p=1,\\ p\neq k}}^{m}\sum_{j=1}^{n_p}(\grave{a}_{pjki} - \acute{a}_{pjki})f_{pj}(x_{pj}(t)) + \sum_{\substack{p=1,\\ p\neq k}}^{m}\sum_{j=1}^{n_p}(\grave{b}_{pjki} - \acute{b}_{pjki})f_{pj}(x_{pj}(t-\tau_{pjki}(t))) + \sum_{\substack{p=1,\\ p\neq k}}^{m}\sum_{j=1}^{n_p}(\grave{c}_{pjki} - \acute{c}_{pjki})\int_{t-\rho(t)}^{t} f_{pj}(x_{pj}(s))ds. \quad (19)$$

Along the trajectory of system (19), we calculate the derivative as follows:

$$\dot{V}(t) \le \Big[-2\grave{d}_{ki} - 2\delta_{ki} + \sum_{\substack{p=1,\\ p\neq k}}^{m}\sum_{j=1}^{n_p}(\grave{a}_{pjki}^2 L_{pj}^2 + \grave{b}_{pjki}^2 L_{pj}^2 + \rho_1 \grave{c}_{pjki}^2 L_{pj}^2 + 1 + \frac{1}{1-\tau_2} + \rho_1)\Big] e_{ki}^2(t) + 2\Big[(\acute{d}_{ki} - \grave{d}_{ki})\Gamma_{ki} + \sum_{\substack{p=1,\\ p\neq k}}^{m}\sum_{j=1}^{n_p}(\grave{a}_{pjki} - \acute{a}_{pjki})L_{pj}\Gamma_{pj} + \sum_{\substack{p=1,\\ p\neq k}}^{m}\sum_{j=1}^{n_p}[(\grave{b}_{pjki} - \acute{b}_{pjki})F + (\grave{c}_{pjki} - \acute{c}_{pjki})\rho_1 F] - \theta_{ki}\Big]|e_{ki}(t)| - h|e_{ki}(t)|^{\eta}. \quad (20)$$

Under the conditions of Theorem 1, we obtain

$$\dot{V}(t) \le -h|e_{ki}(t)|^{\eta}. \quad (21)$$

Then, according to Lemma 2, the drive system (2) and the response system (4) are synchronized in the finite-time $T = t_0 + \frac{V^{1-\eta}(t_0)}{h(1-\eta)}$. This implies the proof is completed.

④ $|x_{ki}(t)| > \Gamma_{ki}$, $|y_{ki}(t)| < \Gamma_{ki}$.

The drive system (2) can be written as system (16), the response system (4) can be written as system (10).

Then the error system is obtained as follows:

$$\begin{aligned}\frac{de_{ki}(t)}{dt} &= \mu_{ki}(t) - \grave{d}_{ki}e_{ki}(t) + \sum_{\substack{p=1,\\ p\neq k}}^{m}\sum_{j=1}^{n_p}\grave{a}_{pjki}\tilde{f}_{pj}(e_{pj}(t)) \\ &+ \sum_{\substack{p=1,\\ p\neq k}}^{m}\sum_{j=1}^{n_p}\grave{b}_{pjki}\tilde{f}_{pj}(e_{pj}(t-\tau_{pjki}(t))) \\ &+ \sum_{\substack{p=1,\\ p\neq k}}^{m}\sum_{j=1}^{n_p}\grave{c}_{pjki}\int_{t-\rho(t)}^{t}\tilde{f}_{pj}(e_{pj}(s))ds \\ &+ (\grave{d}_{ki} - \acute{d}_{ki})y_{ki}(t) \\ &+ \sum_{\substack{p=1,\\ p\neq k}}^{m}\sum_{j=1}^{n_p}(\acute{a}_{pjki} - \grave{a}_{pjki})f_{pj}(y_{pj}(t)) \\ &+ \sum_{\substack{p=1,\\ p\neq k}}^{m}\sum_{j=1}^{n_p}(\acute{b}_{pjki} - \grave{b}_{pjki})f_{pj}(y_{pj}(t-\tau_{pjki}(t))) \\ &+ \sum_{\substack{p=1,\\ p\neq k}}^{m}\sum_{j=1}^{n_p}(\acute{c}_{pjki} - \grave{c}_{pjki})\int_{t-\rho(t)}^{t}f_{pj}(y_{pj}(s))ds. \quad (22)\end{aligned}$$

The proof of the rest is similar to ③, so it is omitted here.

⑤ $|x_{ki}(t)| = \Gamma_{ki}$ or $|y_{ki}(t)| = \Gamma_{ki}$.

The rest of five cases are similar to cases ③ and ④, and the process of proof is omitted here. To sum up, Theorem 1 is proved.

APPENDIX A
PROOF OF THEOREM 2

Construct the following Lyapunov function:

$$V(t) = sign(e_{ki}(t))e_{ki}(t).$$

According to the differential inclusion theorem, Theorem 2 will be proved in nine cases.

① $|x_{ki}(t)| < \Gamma_{ki}$, $|y_{ki}(t)| < \Gamma_{ki}$.

The drive system (2) can be written as system (9), the response system (4) can be written as system (10). Then the error system can be written as system (11).

Along the trajectory of system (11), we calculate the derivative as follows:

$$\begin{aligned}\dot{V}(t) &\le sign(e_{ki}(t))\Big[\mu_{ki}(t) - \acute{d}_{ki}e_{ki}(t) + \sum_{\substack{p=1,\\ p\neq k}}^{m}\sum_{j=1}^{n_p}\acute{a}_{pjki} \\ &\times\tilde{f}_{pj}(e_{pj}(t)) + \sum_{\substack{p=1,\\ p\neq k}}^{m}\sum_{j=1}^{n_p}\acute{b}_{pjki}\tilde{f}_{pj}(e_{pj}(t-\tau_{pjki}(t))) \\ &+ \sum_{\substack{p=1,\\ p\neq k}}^{m}\sum_{j=1}^{n_p}\acute{c}_{pjki}\int_{t-\rho(t)}^{t}\tilde{f}_{pj}(e_{pj}(s))ds\Big]. \quad (23)\end{aligned}$$

Then we obtain

$$\begin{aligned}\dot{V}(t) &\le -\acute{d}_{ki}|e_{ki}(t)| + \sum_{\substack{p=1,\\ p\neq k}}^{m}\sum_{j=1}^{n_p}|\acute{a}_{pjki}\tilde{f}_{pj}(e_{pj}(t))| \\ &+ \sum_{\substack{p=1,\\ p\neq k}}^{m}\sum_{j=1}^{n_p}|\acute{b}_{pjki}\tilde{f}_{pj}(e_{pj}(t-\tau_{pjki}(t)))| \\ &+ \sum_{\substack{p=1,\\ p\neq k}}^{m}\sum_{j=1}^{n_p}|\acute{c}_{pjki}\int_{t-\rho(t)}^{t}\tilde{f}_{pj}(e_{pj}(s))ds| - \delta_{ki}|e_{ki}(t)| \\ &- \theta_{ki}|e_{pj}(t-\tau_{pjki}(t))| - \varepsilon_{ki}|\int_{t-\rho(t)}^{t}e_{pj}(s)ds| \\ &- (\gamma_{ki} + h|e_{ki}(t)|^{\eta}). \quad (24)\end{aligned}$$

According to Assumption 1, we have

$$\begin{aligned}\dot{V}(t) &\le -(\acute{d}_{ki} + \delta_{ki})|e_{ki}(t)| + \sum_{\substack{p=1,\\ p\neq k}}^{m}\sum_{j=1}^{n_p}|\acute{a}_{pjki}L_{pj}e_{pj}(t)| \\ &+ \sum_{\substack{p=1,\\ p\neq k}}^{m}\sum_{j=1}^{n_p}|\acute{b}_{pjki}L_{pj}e_{pj}(t-\tau_{pjki}(t))| \\ &+ \sum_{\substack{p=1,\\ p\neq k}}^{m}\sum_{j=1}^{n_p}|\acute{c}_{pjki}L_{pj}\int_{t-\rho(t)}^{t}e_{pj}(s)ds| \\ &- \theta_{ki}|e_{pj}(t-\tau_{pjki}(t))| - \varepsilon_{ki}|\int_{t-\rho(t)}^{t}e_{pj}(s)ds| \\ &- (\gamma_{ki} + h|e_{ki}(t)|^{\eta}) \\ &\le \sum_{\substack{p=1,\\ p\neq k}}^{m}\sum_{j=1}^{n_p}(-\acute{d}_{ki} + \acute{a}_{pjki}L_{pj} - \delta_{ki})|e_{ki}(t)| \\ &+ \sum_{\substack{p=1,\\ p\neq k}}^{m}\sum_{j=1}^{n_p}(\acute{b}_{pjki}L_{pj} - \theta_{ki})|e_{pj}(t-\tau_{pjki}(t))| \\ &+ \sum_{\substack{p=1,\\ p\neq k}}^{m}\sum_{j=1}^{n_p}(\acute{c}_{pjki}L_{pj} - \varepsilon_{ki})|\int_{t-\rho(t)}^{t}e_{pj}(s)ds| \\ &- h|e_{ki}(t)|^{\eta}. \quad (25)\end{aligned}$$

Under the conditions of Theorem 2, we obtain

$$\dot{V}(t) \le -h|e_{ki}(t)|^{\eta}. \quad (26)$$

Then, according to Lemma 2, the drive system (2) and the response system (4) are synchronized in the finite-time $T = t_0 + \frac{V^{1-\eta}(t_0)}{h(1-\eta)}$. This implies the proof is completed.

② $|x_{ki}(t)| > \Gamma_{ki}$, $|y_{ki}(t)| > \Gamma_{ki}$.

The drive system (2) can be written as system (16), the response system (4) can be written as system (17). Then the error system can be written as system (18). The proof of the rest is similar to ①, so it is omitted here.

③ $|x_{ki}(t)| < \Gamma_{ki}$, $|y_{ki}(t)| > \Gamma_{ki}$.

The drive system (2) can be written as system (9), the response system (4) can be written as system (17). Then the error system can be written as system (19).

Along the trajectory of system (19), we calculate the derivative as follows:

$$\begin{aligned}\dot{V}(t) \le & -\acute{d}_{ki}|e_{ki}(t)| + \sum_{\substack{p=1,\\ p\neq k}}^{m}\sum_{j=1}^{n_p}|\acute{a}_{pjki}\tilde{f}_{pj}(e_{pj}(t))| \\ & + \sum_{\substack{p=1,\\ p\neq k}}^{m}\sum_{j=1}^{n_p}|\acute{b}_{pjki}\tilde{f}_{pj}(e_{pj}(t-\tau_{pjki}(t)))| \\ & + \sum_{\substack{p=1,\\ p\neq k}}^{m}\sum_{j=1}^{n_p}|\acute{c}_{pjki}\int_{t-\rho(t)}^{t}\tilde{f}_{pj}(e_{pj}(s))ds| \\ & + sign(e_{ki}(t))(\acute{d}_{ki}-\grave{d}_{ki})x_{ki}(t) \\ & + sign(e_{ki}(t))\Big[\sum_{\substack{p=1,\\ p\neq k}}^{m}\sum_{j=1}^{n_p}(\grave{a}_{pjki}-\acute{a}_{pjki})f_{pj}(x_{pj}(t)) \\ & + \sum_{\substack{p=1,\\ p\neq k}}^{m}\sum_{j=1}^{n_p}(\grave{b}_{pjki}-\acute{b}_{pjki})f_{pj}(x_{pj}(t-\tau_{pjki}(t))) \\ & + \sum_{\substack{p=1,\\ p\neq k}}^{m}\sum_{j=1}^{n_p}(\grave{c}_{pjki}-\acute{c}_{pjki})\int_{t-\rho(t)}^{t}f_{pj}(x_{pj}(s))ds\Big] \\ & - \delta_{ki}|e_{ki}(t)| - \theta_{ki}|e_{pj}(t-\tau_{pjki}(t))| \\ & - \varepsilon_{ki}|\int_{t-\rho(t)}^{t}e_{pj}(s)ds| - (\gamma_{ki}+h|e_{ki}(t)|^{\eta}). \end{aligned} \tag{27}$$

According to Assumption 1, we have

$$\begin{aligned}\dot{V}(t) \le & \sum_{\substack{p=1,\\ p\neq k}}^{m}\sum_{j=1}^{n_p}(-\acute{d}_{ki}+\acute{a}_{pjki}L_{pj}-\delta_{ki})|e_{ki}(t)| \\ & + \sum_{\substack{p=1,\\ p\neq k}}^{m}\sum_{j=1}^{n_p}(\acute{b}_{pjki}L_{pj}-\theta_{ki})|e_{pj}(t-\tau_{pjki}(t))| \\ & + \sum_{\substack{p=1,\\ p\neq k}}^{m}\sum_{j=1}^{n_p}(\acute{c}_{pjki}L_{pj}-\varepsilon_{ki})|\int_{t-\rho(t)}^{t}e_{pj}(s)ds| \\ & + \Big\{|\acute{d}_{ki}-\grave{d}_{ki}|\Gamma_{ki} + \sum_{\substack{p=1,\\ p\neq k}}^{m}\sum_{j=1}^{n_p}\Big[|\grave{a}_{pjki}-\acute{a}_{pjki}|L_{pj}\Gamma_{pj} \\ & + |\grave{b}_{pjki}-\acute{b}_{pjki}|F + |\grave{c}_{pjki}-\acute{c}_{pjki}|\rho_1 F\Big] - \gamma_{ki}\Big\} \\ & - h|e_{ki}(t)|^{\eta}. \end{aligned} \tag{28}$$

Under the conditions of Theorem 2, we obtain

$$\dot{V}(t) \le -h|e_{ki}(t)|^{\eta}. \tag{29}$$

Then, according to Lemma 2, the drive system (2) and the response system (4) are synchronized in the finite-time $T = t_0 + \frac{V^{1-\eta}(t_0)}{h(1-\eta)}$. This implies the proof is completed.

④ $|x_{ki}(t)| > \Gamma_{ki}$, $|y_{ki}(t)| < \Gamma_{ki}$.

The drive system (2) can be written as system (16), the response system (4) can be written as system (10). Then the error system can be written as system (22). The proof of the rest is similar to ③, so it is omitted here.

⑤ $|x_{ki}(t)| = \Gamma_{ki}$ or $|y_{ki}(t)| = \Gamma_{ki}$.

The rest of five cases are similar to cases ③ and ④, and the process of proof is omitted here. To sum up, Theorem 2 is proved.

REFERENCES

[1] Ü. Çavuşoğlu, S. Kaçar, I. Pehlivan, and A. Zengin, "Secure image encryption algorithm design using a novel chaos based S-Box," *Chaos, Solitons Fractals*, vol. 95, pp. 92–101, Feb. 2017, doi: 10.1016/j.chaos.2016.12.018.

[2] A. Kanso and M. Ghebleh, "An algorithm for encryption of secret images into meaningful images," *Opt. Lasers Eng.*, vol. 90, pp. 196–208, Mar. 2017, doi: 10.1016/j.optlaseng.2016.10.009.

[3] Y. Zhang, "A chaotic system based image encryption scheme with identical encryption and decryption algorithm," *Chin. J. Electron.*, vol. 26, pp. 1022–1031, Sep. 2017, doi: 10.1049/cje.2017.08.022.

[4] R. Parvaz and M. Zarebnia, "A combination chaotic system and application in color image encryption," *Opt. Laser Technol.*, vol. 101, pp. 30–41, May 2018, doi: 10.1016/j.optlastec.2017.10.024.

[5] N. Bigdeli, Y. Farid, and K. Afshar, "A novel image encryption/decryption scheme based on chaotic neural networks," *Eng. Appl. Artif. Intell.*, vol. 25, pp. 753–765, Jun. 2012.

[6] K. Ratnavelu, M. Kalpana, P. Balasubramaniam, K. Wong, and P. Raveendran, "Image encryption method based on chaotic fuzzy cellular neural networks," *Signal Process.*, vol. 140, pp. 87–96, Nov. 2017, doi: 10.1016/j.sigpro.2017.05.002.

[7] S. Zhou, "Image encryption technology research based on neural network," in *Proc. Int. Conf. Intell. Transp., Big Data Smart City (ICITBS)*, Dec. 2015, pp. 19–20, doi: 10.1109/ICITBS.2015.119.

[8] M. Prakash, P. Balasubramaniam, and S. Lakshmanan, "Synchronization of Markovian jumping inertial neural networks and its applications in image encryption," *Neural Netw.*, vol. 83, pp. 86–93, Nov. 2016, doi: 10.1016/j.neunet.2016.07.001.

[9] S. Wen, Z. Zeng, T. Huang, Q. Meng, and W. Yao, "Lag synchronization of switched neural networks via neural activation function and applications in image encryption," *IEEE Trans. Neural Netw. Learn. Syst.*, vol. 26, no. 7, pp. 1493–1502, Jul. 2015, doi: 10.1109/TNNLS.2014.2387355.

[10] X. Zhang, S. Sheng, G. Lu, and Y. Zheng, "Synchronization for arrays of coupled jumping delayed neural networks and its application to image encryption," in *Proc. IEEE 56th Annu. Conf. Decis. Control (CDC)*, Dec. 2017, pp. 12–15, doi: 10.1109/CDC.2017.8263821.

[11] X. Chai, Z. Gan, K. Yang, Y. Chen, and X. Liu, "An image encryption algorithm based on the memristive hyperchaotic system, cellular automata and DNA sequence operations," *Signal Process., Image Commun.*, vol. 52, pp. 6–19, Mar. 2017, doi: 10.1016/j.image.2016.12.007.

[12] B. Wang, F. C. Zou, and J. Cheng, "A memristor-based chaotic system and its application in image encryption," *Optik—Int. J. Light Electron Opt.*, vol. 154, pp. 538–544, Feb. 2018, doi: 10.1016/j.ijleo.2017.10.080.

[13] J. Lu and D. W. Ho, "Stabilization of complex dynamical networks with noise disturbance under performance constraint," *Nonlinear Anal. Real World Appl.*, vol. 12, no. 4, pp. 1974–1984, 2011, doi: 10.1016/j.nonrwa.2010.12.013.

[14] X. Huang, Y. J. Fan, J. Jia, Z. Wang, and Y. Li, "Quasi-synchronisation of fractional-order memristor-based neural networks with parameter mismatches," *IET Control Theory Appl.*, vol. 11, pp. 2317–2327, Sep. 2017, doi: 10.1049/iet-cta.2017.0196.

[15] Y. V. Pershin and M. Di Ventra, "Experimental demonstration of associative memory with memristive neural networks," *Neural Netw.*, vol. 23, no. 7, pp. 881–886, 2010, doi: 10.1016/j.neunet.2010.05.001.

[16] M. Itoh and L. O. Chua, "Memristor cellular automata and memristor discrete-time cellular neural networks," *Int. J. Bifurcation Chaos*, vol. 19, no. 11, pp. 3605–3656, Nov. 2009, doi: 10.1142/S0218127409025031.
[17] M. Zheng *et al.*, "Finite-time stability and synchronization of memristor-based fractional-order fuzzy cellular neural networks," *Commun. Nonlinear Sci. Numer. Simul.*, vol. 59, pp. 272–291, Jun. 2018, doi: 10.1016/j.cnsns.2017.11.025.
[18] J. Chen, C. Li, T. Huang, and X. Yang, "Global stabilization of memristor-based fractional-order neural networks with delay via output-feedback control," *Modern Phys. Lett. B*, vol. 31, pp. 1–19, Feb. 2017, doi: 10.1142/S0217984917500312.
[19] M. Yu, W. Wang, X. Luo, L. Liu, and M. Yuan, "Exponential anti-synchronization control of stochastic memristive neural networks with mixed time-varying delays based on novel delay-dependent or delay-independent adaptive controller," *Math. Problems Eng.*, vol. 2017, Mar. 2017, Art. no. 8314757, doi: 10.1155/2017/8314757.
[20] J. Yang, L. Wang, Y. Wang, and T. Guo, "A novel memristive Hopfield neural network with application in associative memory," *Neurocomputing*, vol. 227, pp. 142–148, Mar. 2016, doi: 10.1016/j.neucom.2016.07.065.
[21] S. Zhu, L. Wang, and S. Duan, "Memristive pulse coupled neural network with applications in medical image processing," *Neurocomputing*, vol. 227, pp. 149–157, Mar. 2017, doi: 10.1016/j.neucom.2016.07.068.
[22] X. Hu, G. Feng, S. Duan, and L. Liu, "A memristive multilayer cellular neural network with applications to image processing," *IEEE Trans. Neural Netw. Learn. Syst.*, vol. 28, no. 8, pp. 1889–1901, Aug. 2016, doi: 10.1109/TNNLS.2016.2552640.
[23] C. Chen, L. Li, H. Peng, and Y. Yang, "Fixed-time synchronization of memristor-based BAM neural networks with time-varying discrete delay," *Neural Netw.*, vol. 96, pp. 47–54, Dec. 2017, doi: 10.1016/j.neunet.2017.08.012.
[24] M. Zheng, L. Li, H. Peng, J. Xiao, Y. Yang, and Y. Zhang, "Fixed-time synchronization of memristive fuzzy BAM cellular neural networks with time-varying delays based on feedback controllers," *IEEE Access*, vol. 6, pp. 12085–12102, 2018, doi: 10.1109/ACCESS.2018.2805183.
[25] R. Sakthivel, R. Anbuvithya, K. Mathiyalagan, Y.-K. Ma, and P. Prakash, "Reliable anti-synchronization conditions for BAM memristive neural networks with different memductance functions," *Appl. Math. Comput.*, vol. 275, pp. 213–228, Feb. 2016, doi: 10.1016/j.amc.2015.11.060.
[26] W. Wang, M. Yu, X. Luo, L. Liu, M. Yuan, and W. Zhao, "Synchronization of memristive BAM neural networks with leakage delay and additive time-varying delay components via sampled-data control," *Chaos Solitons Fractals*, vol. 104, pp. 84–97, Nov. 2017, doi: 10.1016/j.chaos.2017.08.011.
[27] C. Chen, L. Li, H. Peng, and Y. Yang, "Adaptive synchronization of memristor-based BAM neural networks with mixed delays," *Appl. Math. Comput.*, vol. 322, pp. 100–110, Apr. 2018, doi: 10.1016/j.amc.2017.11.037.
[28] M. Hagiwara, "Multidirectional associative memory," in *Proc. Int. Joint Conf. Neural Netw.*, vol. 1, 1990, pp. 3–6.
[29] S.-C. Chen and H. Gao, "Multivalued exponential multidirectional associative memory," *J. Softw.*, vol. 9, pp. 397–400, May 1998.
[30] M. Wang, T. Zhou, and X. Zhang, "Global exponential stability of discrete-time multidirectional associative memory neural network with variable delays," *ISRN Discrete Math.*, vol. 2012, Sep. 2012, Art. no. 831715, doi: 10.5402/2012/831715.
[31] P. Basaras, G. Iosifidis, D. Katsaros, and L. Tassiulas, "Identifying influential spreaders in complex multilayer networks: A centrality perspective," *IEEE Trans. Netw. Sci. Eng.*, to be published, doi: 10.1109/TNSE.2017.2775152.
[32] P. Jiang, Z. Zeng, and J. Chen, "On the periodic dynamics of memristor-based neural networks with leakage and time-varying delays," *Neurocomputing*, vol. 219, pp. 163–173, Jan. 2017, doi: 10.1016/j.neucom.2016.09.029.
[33] A. Wu and Z. Zeng, "Lagrange stability of memristive neural networks with discrete and distributed delays," *IEEE Trans. Neural Netw. Learn. Syst.*, vol. 25, no. 4, pp. 690–703, Apr. 2014, doi: 10.1109/TNNLS.2013.2280458.
[34] W. Wang *et al.*, "Anti-synchronization of coupled memristive neutral-type neural networks with mixed time-varying delays via randomly occurring control," *Nonlinear Dyn.*, vol. 83, pp. 2143–2155, Mar. 2016, doi: 10.1007/s11071-015-2471-9.
[35] O. M. Kwon, J. H. Park, and S. M. Lee, "Secure communication based on chaotic synchronization via interval time-varying delay feedback control," *Nonlinear Dyn.*, vol. 63, pp. 239–252, Jan. 2011, doi: 10.1007/s11071-010-9800-9.
[36] H. Tirandaz and A. Karmi-Mollaee, "Modified function projective feedback control for time-delay chaotic Liu system synchronization and its application to secure image transmission," *Optik—Int. J. Light Electron Opt.*, vol. 147, pp. 187–196, Oct. 2017, doi: 10.1016/j.ijleo.2017.08.103.
[37] X. Luo, J. Deng, J. Liu, W. Wang, X. Ban, and J.-H. Wang, "A quantized kernel least mean square scheme with entropy-guided learning for intelligent data analysis," *China Commun.*, vol. 14, no. 7, pp. 1–10, Jul. 2017.
[38] J. Chen, Z. Zeng, and P. Jiang, "Global Mittag-Leffler stability and synchronization of memristor-based fractional-order neural networks," *Neural Netw.*, vol. 51, pp. 1–8, Mar. 2014, doi: 10.1016/j.neunet.2013.11.016.
[39] C. Chen, L. Li, H. Peng, Y. Yang, and T. Li, "Finite-time synchronization of memristor-based neural networks with mixed delays," *Neurocomputing*, vol. 235, pp. 83–89, Apr. 2017, doi: 10.1016/j.neucom.2016.12.061.
[40] Z. Cai, L. Huang, M. Zhu, and D. Wang, "Finite-time stabilization control of memristor-based neural networks," *Nonlinear Anal., Hybrid Syst.*, vol. 20, pp. 37–54, May 2016, doi: 10.1016/j.nahs.2015.12.001.
[41] L. Wang, Q. Song, Y. Liu, Z. Zhao, and F. E. Alsaadi, "Finite-time stability analysis of fractional-order complex-valued memristor-based neural networks with both leakage and time-varying delays," *Neurocomputing*, vol. 245, pp. 86–101, Jul. 2017, doi: 10.1016/j.neucom.2017.03.042.
[42] A. Wu and Z. Zeng, "Anti-synchronization control of a class of memristive recurrent neural networks," *Commun. Nonlinear Sci. Numer. Simul.*, vol. 18, no. 2, pp. 373–385, 2013, doi: 10.1016/j.cnsns.2012.07.005.
[43] A. Wu, S. Wen, and Z. Zeng, "Synchronization control of a class of memristor-based recurrent neural networks," *Inf. Sci.*, vol. 183, no. 1, pp. 106–116, 2012, doi: 10.1016/j.ins.2011.07.044.
[44] X. Y. Niu, "Applications of image encryption under multiple chaotic sequences," M.S. thesis, Dept. Commun. Inf. Syst., Heilongjiang Univ., Heilongjiang, China, 2014.

WEIPING WANG received the Ph.D. degree in telecommunications physics electronics from the Beijing University of Posts and Telecommunications, Beijing, China, in 2015. She is currently an Associate Professor with the Department of Computer and Communication Engineering, University of Science and Technology Beijing. She received the National Natural Science Foundation of China, the Post-Doctoral Fund, and the basic scientific research project. Her current research interests include brain-like computing, memristive neural network, associative memory awareness simulation, complex network, network security, and image encryption.

XIN YU received the bachelor's degree in computer science and technology from Yanshan University, Hebei, China, in 2016. She is currently pursuing the M.E. degree with the University of Science and Technology Beijing, Beijing, China. Her current research interests include memristive neural networks and brain computing.

XIONG LUO (M'16) received the Ph.D. degree in computer applied technology from Central South University, Changsha, China, in 2004. He is currently a Professor with the School of Computer and Communication Engineering, University of Science and Technology Beijing, Beijing, China. His current research interests include neural networks, machine learning, and computational intelligence. He has authored extensively in his areas of interest in several journals, such as the IEEE ACCESS, *Future Generation Computer Systems*, and *Personal and Ubiquitous Computing*.

JÜRGEN KURTHS studied mathematics with the University of Rostock and received the Ph.D. degree from the GDR Academy of Sciences in 1983. He was a Full Professor with the University of Potsdam from 1994 to 2008. He has been a Professor of nonlinear dynamics with Humboldt University, Berlin, and the Chair of the research domain transdisciplinary concepts of the Potsdam Institute for Climate Impact Research since 2008 and a Sixth-Century Chair of Aberdeen University, U.K., since 2009. He has authored over 500 papers that are cited over 18 000 times (h-factor: 57). His primary research interests include synchronization, complex networks, and time series analysis and their applications. He is a fellow of the American Physical Society. He became a member of the Academia Europaea in 2010 and the Macedonian Academy of Sciences and Arts in 2012. He received the Alexander von Humboldt Research Award from CSIR, India, in 2005, and an Honorary Doctorate from the Lobachevsky University Nizhny Novgorod in 2008 and one from the State University Saratov in 2012. He is an Editor of journals, such as PLoS ONE, the *Philosophical Transaction of the Royal Society A*, the *Journal of Nonlinear Science*, and *Chaos*.